Radiología. 2019;61(2):99–123

RADIOLOGÍA

www.elsevier.es/rx

UPDATE IN RADIOLOGY

Cranial nerve disorders: Clinical manifestations and topography☆

M. Jorquera Moya[a,*], S. Merino Menéndez[a], J. Porta Etessam[b], J. Escribano Vera[c], M. Yus Fuertes[a]

[a] *Sección de Neurorradiología, Hospital Clínico San Carlos, Madrid, Spain*
[b] *Servicio de Neurología, Hospital Clínico San Carlos, Madrid, Spain*
[c] *Neurorradiología, Hospital Ruber Internacional, Madrid, Spain*

Received 17 November 2017; accepted 27 September 2018

KEYWORDS
Cranial pairs;
Cranial nerves;
Cranial neuropathies;
Neuralgia;
Cranial nerve palsy

Abstract The detection of pathological conditions related to the twelve cranial pairs represents a significant challenge for both clinicians and radiologists; imaging techniques are fundamental for the management of many patients with these conditions. In addition to knowledge about the anatomy and pathological entities that can potentially affect the cranial pairs, the imaging evaluation of patients with possible cranial pair disorders requires specific examination protocols, acquisition techniques, and image processing.

This article provides a review of the most common symptoms and syndromes related with the cranial pairs that might require imaging tests, together with a brief overview of the anatomy, the most common underlying processes, and the most appropriate imaging tests for different indications.
© 2018 SERAM. Published by Elsevier España, S.L.U. All rights reserved.

PALABRAS CLAVE
Pares craneales;
Nervios craneales;
Neuropatía de pares craneales;
Neuralgia;
Parálisis

Sintomatología derivada de los pares craneales: Clínica y topografía

Resumen La detección de la patología relacionada con los doce pares craneales representa un importante desafío, tanto para los clínicos como para los radiólogos. Las técnicas de imagen son fundamentales para el manejo de muchos de los pacientes. Adicionalmente al conocimiento anatómico y de las entidades patológicas que potencialmente puedan afectarlos, la evaluación por imagen de los pares craneales requiere protocolos de exploración y técnicas de adquisición y procesado específicas.

☆ Please cite this article as: Jorquera Moya M, Merino Menéndez S, Porta Etessam J, Escribano Vera J, Yus Fuertes M. Sintomatología derivada de los pares craneales: Clínica y topografía. Radiología. 2019;61:99–123.

* Corresponding author.
E-mail address: manuela.jorquera@gmail.com (M. Jorquera Moya).

2173-5107/© 2018 SERAM. Published by Elsevier España, S.L.U. All rights reserved.

En este artículo se efectúa un repaso de los principales síntomas y síndromes relacionados con los nervios craneales que pueden precisar la realización de pruebas de imagen y la patología subyacente, así como una breve revisión de la anatomía y de las técnicas de imagen más adecuadas a la indicación.
© 2018 SERAM. Publicado por Elsevier España, S.L.U. Todos los derechos reservados.

Anatomy of memory

There are 12 pairs of cranial nerves that connect the brain stem with structures of the head and neck and the thoracic and abdominal cavities. Table 1 summarises the anatomical course of cranial nerves III to XII.

There are three types according to their function: sensory, motor and mixed nerves. Table 2 lists the nomenclature, function and clinical semiology of the cranial nerves.

In each cranial nerve, the intra-axial (nucleus and fascicle), cisternal, dural and interdural, bony or foraminal and extraforaminal segments are differentiated.[1] The *nuclei* are distributed from the midbrain to the proximal cervical cord.

The *cisternal segment* has two parts, a central one, myelinated by oligodendrocytes, and a peripheral one whose myelin is formed by Schwann cells. Between both segments is the transition or Steiner-Redlich zone, variable from one pair to another, more vulnerable to neurovascular compression and threshold for the location of schwannomas (distal to this).

In some nerves, a *dural segment* can be identified, located in a dural evagination with cerebrospinal fluid (CSF) content such as Meckel's *cave*.

The *interdural segment* is located between two dura mater sheets and is occupied by venous plexuses such as the cavernous sinus.

The *foraminal segment*, also surrounded by venous plexuses, is located at the base of the skull.

The *extraforaminal segment* corresponds to the extracranial nerve course.

Imaging techniques

Magnetic resonance imaging (MRI) is the technique of choice for the evaluation of cranial nerves.

The intra-axial segment can be evaluated by means of the usual sequences for the study of the brain. The remaining segments require specific sequences, and these are the SSFP (Steady-State Free Precession), named as 3D FIESTA/CISS, Fast Imaging Employing Steady-state Acquisition/Constructive Interference Steady State sequences, which demonstrate the cranial nerves in their cisternal path, and when post-contrast has been performed, the interdural and foraminal trajectories by the enhancement of the venous plexuses.[2–4]

The 3D FLAIR sequence makes it possible to see the cistern segments and the detection of post-contrast enhancements in these and in the meninges.[5,6]

The 2D FSE T1, T1 post-contrast and T2 with fat suppression and post-contrast sequences 3D T1 with fat suppression make it possible to evaluate the cisternal, foraminal and extraforaminal segments, and the course in the craniofacial region of the terminal branches of the cranial nerves.

In neurovascular compression syndromes, angiographic sequences are useful, mainly 3D TOF. The visualisation of the images co-registered with the FIESTA/CISS sequence facilitates the interpretation of the findings.[7] The sequences of time-resolved imaging of contrast kinetics (TRICKS) are especially indicated when a dural fistula or AVM is suspected.[8]

The nerves of greater section allow for their microstructural evaluation by means of diffusion tensor sequencing.[9] Tractography can be useful in locating some of the nerves that are difficult to identify in the case of expansive processes.[10] Table 3 summarises the main sequences that must be performed in case of pathology of the cranial nerves.

Computed tomography (CT) complements magnetic resonance imaging (MRI), which allows us to evaluate the foramina and intraosseous trajectories of the cranial nerves at the base of the skull, especially the petrous apex (Figs. 1 and 2).

Semiology and pathology of cranial nerves I and II

Nerves I (olfactory nerve) and II (optic nerve) are considered prolongations of white matter tracts of the central nervous system. They do not follow the anatomical classification or division into the same segments as the rest of the cranial nerves; nor do they share the same pathology, so clinical semiology and pathology will be dealt with separately.

Olfactory disorders

The olfactory nerve consists of a set of unmyelinated nerve fillets that arise from the olfactory portion of the pituitary mucosa in the roof of the nostril; said fillets cross the lamina cribrosa and end in the ventral region of the *olfactory bulb* where they synapse with the second neuron (Fig. 1). The efferent axons leave the olfactory bulb and reach the olfactory cortex through the olfactory tract.

Anosmia can occur due to injury at any location of the olfactory pathway. When it is unilateral, the location is proximal to the piriform cortex. The most common causes are

Table 1 Anatomy of the cranial nerves.

Cranial nerve	Nucleus	Apparent source	Cisternal segment	Dural/interdural segment	Foraminal segment	Extracranial segment
III nerve Common ocular motor nerve	Midbrain anterior to aqueduct, at the level of the superior quadrigeminal tubercle	Interpeduncular fossa	Interpeduncular and prepontine cistern Between posterior cerebral arteries (upper) and superior cerebellar arteries (lower)	Cavernous sinus: upper region of the lateral wall	Superior orbital fissure	Orbital apex: annulus of Zinn It is divided into upper and lower branches
IV nerve Trochlear nerve	Midbrain: dorsal to MLF and ventral to periaqueductal grey matter at the level of the inferior quadrigeminal tubercle	Dorsal surface inferior to contralateral quadrigeminal tubercle	Ambient and quadrigeminal cistern up to the margin of the tentorium	Cavernous sinus: inferior lateral wall to III nerve	Superior orbital fissure	Orbital apex: annulus of Zinn
V nerve Trigeminal nerve	1 motor N: lateral pontine tegmentum 3 sensory N: from midbrain to C3	Lateral region of the pons	Prepontine cistern	Meckel's *Cave* Division into three sensitive branches: • V1 ophthalmic – lateral wall of the cavernous sinus • V2 maxillary – lateral wall of the cavernous sinus • V3 mandibular joins the motor root	V1: superior orbital fissure V2: greater foramen rotundum V3: foramen ovale	V1: orbit Branches: lacrimal, frontal and nasociliary n. V2: pterygopalatine fossa-orbit through inferior orbital fissure V3 + motor branch: chewing space
VI nerve External ocular motor	Pons near the midline at the level of the tubercle of the facial nerve that protrudes the floor of IV ventricle	Bulboprotuberancial groove	Superior course in prepontine cistern	Dorello's canal on the back of the clivus Then inside of medial cavernous sinus to V1	Superior orbital fissure	Orbit: external rectus muscle
VII nerve Facial nerve	Ventrolateral pontine tegmentum Sensory n.: n. of the solitary tract Parasympathetic n.: superior salivary	Bulboprotuberancial groove 2 nerves: facial (motor) and intermediate (sensory and parasympathetic)	Cerebellopontine angle cistern	Intratemporal • IAC • Labyrinthine s. • Tympanic s. • Mastoid s.	Stylomastoid foramen	Parotid lateral to the retromandibular vein

Table 1 (*Continued*)

Cranial nerve	Nucleus	Apparent source	Cisternal segment	Dural/interdural segment	Foraminal segment	Extracranial segment
VIII nerve Auditory nerve	Lower region of the pons at the level of the IV ventricle	Bulboprotuberancial groove Posterior to the VII nerve Three components: superior vestibular, inferior vestibular and cochlear	Cerebellopontine angle cistern parallel and posterior to the VII nerve	Spiral and vestibular ganglion	IAC: • Cochlear: anterior inferior • Superior vestibular: posterior superior • Inferior vestibular: posterior inferior	
IX nerve Glossopharyngeal nerve	Upper and middle region of the medulla oblongata Motor f.: Ambiguous n. Parasympathetic f.: Inferior salivary n. Sensory f.: Solitary and spinal n. of the trigeminal	Top third of the postolivary groove	Lateral bulbo-cerebellar cistern		Jugular foramen (*pars nervosa*) through the glossopharyngeal meatus Form the upper and lower ganglia	Nasopharyngeal carotid space Bottom of tongue
X nerve Vagus nerve	Upper and middle region of the medulla oblongata Ambiguous and dorsal vagus nuclei in IV ventricle floor	Upper third of the postolivary groove flow to the IX nerve	Lateral bulbo-cerebellar cistern		Jugular foramen (*pars vascularis*) through the vagal meatus	Nasopharyngeal carotid space. Retro-styloid space Superior mediastinum
XI nerve Spinal accessory nerve	Ambiguous nucleus, origin of the cranial root, and anterior horns of the first five cervical segments origin of the spinal root	Lateral groove of the bulb and anterior horns of the spinal cord	Basal cistern		Jugular foramen (*pars vascularis*) through the vagal meatus. It joins to the X nerve	Nasopharyngeal carotid space Subparotid space Sternocleidomastoid and trapezius muscles
XII nerve Hypoglossal nerve	Posterior region of the medulla oblongata in the triangle of the hypoglossal nerve at the level of the floor of the IV ventricle	Preolivary groove	Prebulb cistern		Hypoglossal canal	Carotid space It joins X and XI below the jugular foramen

IAC: internal auditory canal; MLF: medial longitudinal fasciculus.

Table 2 Function of the cranial nerves and clinical semiology.

Cranial nerve	Name	Type	Function/innervation	Clinical semiology
I nerve	Olfactory nerve	Sensory	Smell	Anosmia Hyposmia Hyperosmia
II nerve	Optic nerve	Sensory	Vision	Decreased visual acuity Changes in perception of colours Mononuclear campimetric defects Afferent pupillary defect Abnormalities in the optic disc (oedema, pallor, etc.)
III nerve	Oculomotor nerve	Motor	Eye movements: upper, inner and lower rectus muscles and the upper eyelid lift Parasympathetic fibres in the periphery of the nerve: muscle of the sphincter of the pupil and ciliary muscle (constriction of the pupil and accommodation of the lens)	Diplopia Ptosis Mydriasis
IV nerve	Trochlear nerve	Motor	Superior oblique muscle	Difficulty for downward movement of the eyeball Vertical diplopia
V nerve	Trigeminal nerve		It carries sensory information from:	Anaesthesia, pain or burning in the regions supplied by each branch
	V1 ophthalmic	Sensory	• Scalp and forehead, upper eyelid, cornea, nose, nasal mucosa, frontal sinuses and parts of the meninges	Absence of corneal reflex (nasociliary nerve)
	V2 maxillary	Sensory		Weakness of the chewing muscles and can lead to serous otitis media due to dysfunction of the eustachian tube (eardrum tensor)
	V3 mandibular	Mixed	• Lower eyelid and cheek, back and tip of the nose, upper lip, upper teeth, nasal mucosa, palate and pharyngeal roof, maxillary, ethmoidal and sphenoid sinuses • Lower lip, lower teeth, wings of the nose, chin, pain and temperature of the mouth. The sensitivity of the anterior two thirds of the tongue accompanies a branch of this nerve, the lingual, although these types of nerve fibres then deviate to be part of the VII nerve. Motor function: • Muscles of chewing, mylohyoid, anterior belly of the digastric, tensor of the soft palate and tensor of the eardrum	
VI nerve	External ocular motor	Motor	External rectus muscle	Horizontal diplopia

Table 2 (*Continued*)

Cranial nerve	Name	Type	Function/innervation	Clinical semiology
VII nerve	Facial nerve	Mixed	Parasympathetic I. (secretory and vasodilator fibres): submandibular, sublingual, and lacrimal glands, sweat of the face of the auditory artery and its branches, and the vessels of the nasopharyngeal palate mucous membranes and nostrils Sensory I.: taste perception of the back two thirds of the tongue, sensitivity of the skin of the back of the ear and external auditory canal Motor I.: muscles of facial expression, the stirrup, stylohyoid and posterior belly of the digastric muscle	Facial paralysis: falling facial muscles on the same side of the affected nerve with difficulty in facial expression Pain around the jaw or behind the ear, increased sensitivity to sound, decreased taste Headache and changes in salivation and production of tears Hemifacial spasm: unilateral, involuntary, paroxysmal and repeated contraction (tonic or clonic) of the muscles innervated by the facial nerve
VIII nerve	Auditory or vestibulocochlear	Sensory	Cochlear nerve: hearing Vestibular nerve: balance	Hearing loss, vertigo, tinnitus Vestibular paroxysmia: transient episodes of paroxysmal vertigo, impaired gait and sensation of pressure around the ear, tinnitus or unilateral hearing loss
IX nerve	Glossopharyngeal nerve	Mixed	General sensory of the mucosa of the pharynx, the palatine tonsils, the back third of the tongue, the auditory tube and the middle ear Sensitive for blood pressure and chemistry of the breast and carotid body Motor and proprioceptive for the stylopharyngeus Parasympathetic (secretomotor) for the parotid gland	Neuralgia Paroxysmal pain in the back of the tongue, tonsillar fossa, pharynx, angle of the jaw and/or ear
X nerve	Vagus nerve	Mixed	Sensory I.: tonsillar region, back of the nose and throat, larynx, ear, stomach Parasympathetic I.: heart, bronchi, stomach, oesophagus, intestine, pancreas or liver Motor I.: larynx (recurrent laryngeal nerve and superior laryngeal nerve)	Dysphonia and dysphagia
XI nerve	Spinal accessory nerve	Motor	Sternocleidomastoid and trapezius muscles	Drop of the affected shoulder and weakness of head support Less than 6 months of progression: atrophy of the ipsilateral muscles More than 6 months: compensatory hypertrophy of the levator scapulae muscle on the same side
XII nerve	Hypoglossal nerve	Motor	Intrinsic and extrinsic muscles of the tongue (styloglossus, hyoglossus, genioglossus)	Loss of volume of the tongue, reduced number of papillae, deviation of this to the pathological side

Table 3 Magnetic resonance sequences useful in cranial nerve pathology.

Sequence	Plane	Type	Comments
Diffusion	Axial	2D	Detection of ischaemic pathology
T2*/SWI	Axial	2D/3D	Detection of parenchymal haemorrhage or superficial siderosis
FLAIR	Axial (sagittal)	2D (3D)	3D acquisition preferred if available
T2 FSE/TSE	Coronal (sagittal)	2D (3D)	Fat saturation. 3D acquisition preferred if available
T1 FSE/TSE	Axial and coronal	2D	Fat saturation if there is a suspicion of carotid dissection
FIESTA/CISS	Axial	3D	Positioning according to the clinically affected nerve
TOF	Axial	3D	Optional in case of suspicion of vascular compression syndrome
TRICKS	Axial	3D	Optional in case of suspicion of skull base fistula
STIR	Coronal	2D	Optional in case of suspicion of pathology of the optic nerve
T1 FSE/TSE (+GD)	Axial and coronal	2D	Fat saturation
FIESTA/CISS (+GD)	Axial	3D	Important in evaluation of lower nerves and with intracavernosal path
T1 GR/FSE (+GD)	Axial	3D	Fat saturation. High-resolution volumetric acquisition
FLAIR (+GD)	Axial (sagittal)	2D (3D)	3D acquisition preferred if available

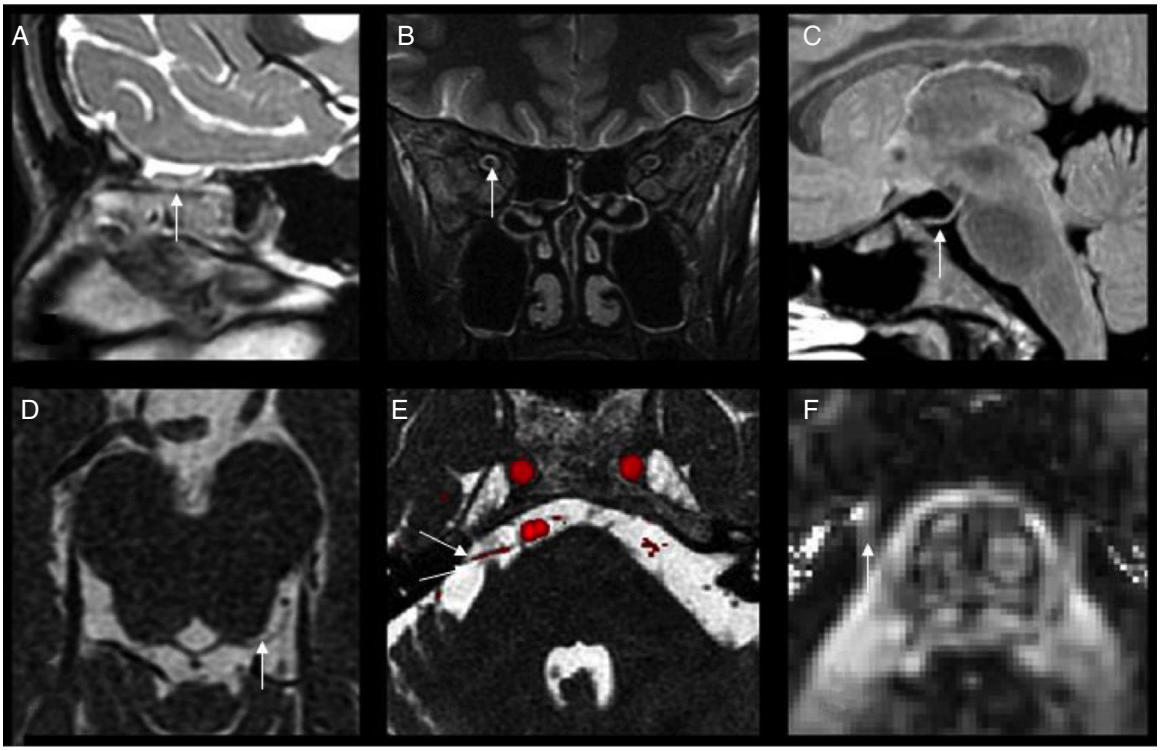

Figure 1 Technique and anatomy. (A) 3D sagittal sequence FSE T2 showing the olfactory bulb (arrow). (B) Coronal STIR sequence where the optic nerve is seen in its intraorbital path (arrow). (C) Oblique reformatting of the 3D FLAIR sequence showing the cisternal path of the III nerve (arrow). (D) 3D FIESTA sequence axial slice 0.3 mm thick, showing part of the cisternal path of the IV nerve (arrow). (E) 3D FIESTA and 3D TOF sequence fusion, which highlights the cisternal segment of the V nerve, with a blood vessel in its proximity (arrow). (F) Fractional anisotropy map, derived from the diffusion tensor sequence, where the V nerve is visualised in its cisternal path (arrow).

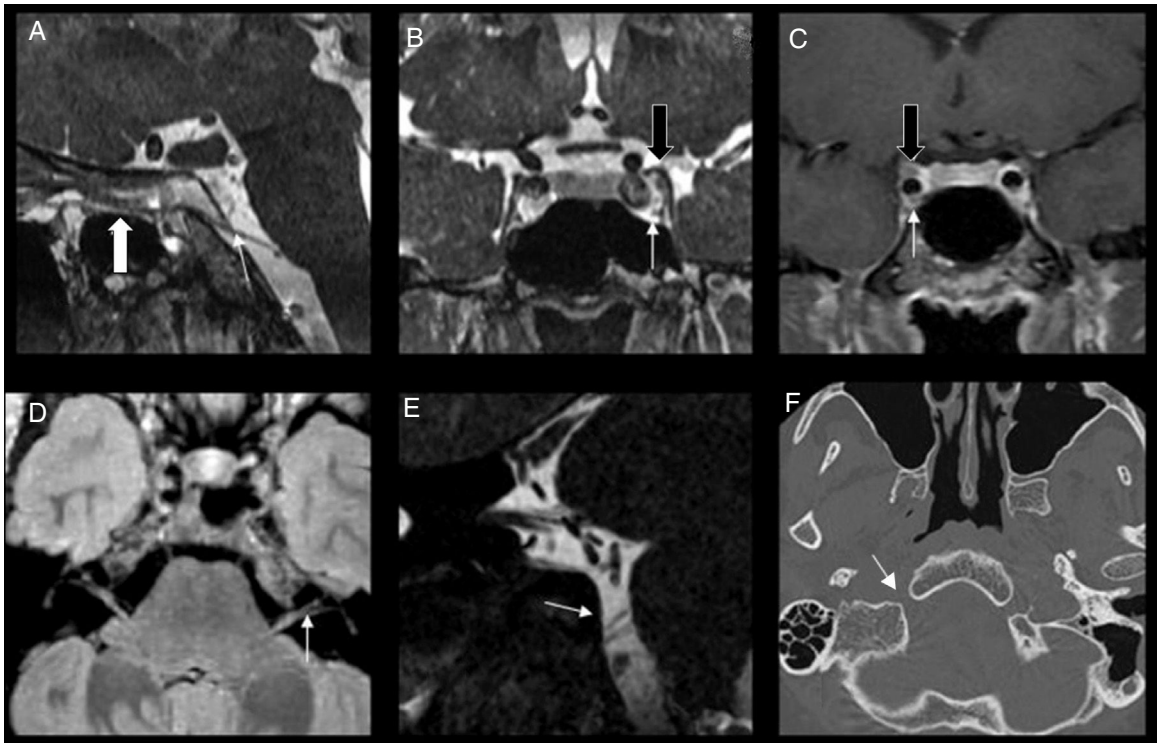

Figure 2 Technique and anatomy. (A) Sagittal reformatting of the 3D FIESTA post-contrast sequence, where the entire VI nerve path is observed in its cisternal and intradural segments (thin and thick arrows). (B and C) Coronal section of 3D FIESTA sequence reformatting and FSE sequence enhanced in T1 post-contrast and with fat suppression, where the III and VI nerves are observed in their intracavernosal path (thick and thin arrows, respectively). (D) Axial reformatting of the 3D FLAIR sequence showing the path of the VII and VIII nerves at cerebellopontine angle and internal auditory canal (arrow). (E) Oblique reformatting of the 3D FIESTA sequence where nerve roots are observed corresponding to IX, X, XI nerves (arrow). (F) Computed tomography (axial section) showing the bone canal of the XII nerve (arrow).

sinonasal inflammatory pathology and trauma of the base of the skull.[11]

Esthesioneuroblastoma, or olfactory neuroblastoma, is a rare tumour in older adults that derives from the basal cells of the olfactory mucosa. Patients may present with nasal congestion, epistaxis, anosmia and headache. They tend to be large tumours at diagnosis. Although there is usually microscopic dural involvement, in 30% the intracranial invasion is clear, and in these cases non-tumour cysts are common in the tumour-brain parenchyma interface (Fig. 3).[12]

Other causes of anosmia in the conductive pathway are neoplasms of the nasal cavity and paranasal sinuses, toxic substances such as cocaine and tobacco and, in the central sensorineural area, Kallmann syndrome, infections, meningioma, surgery and radiation. Hyposmia is also common in the early stages of Alzheimer's and Parkinson's diseases.[13]

Optic neuropathy

It is characterised by specific signs and symptoms shown in Table 2.

The optic pathway includes the optic nerves, the chiasm and the retrochiasmatic structures (Fig. 4).

In the optic nerve several segments are distinguished: *intraocular* (formed by the axons of ganglion cells of the retina), *intraorbital* (intraconal, surrounded by meninges), *intracanalicular* (in the optic canal) and *intracranial* (10 mm before the chiasm, coated only by pia mater). The optic nerves join to form the chiasm where the fibres of the nasal retina of each nerve decussate and join the fibres of the temporal retina not discussed to form the *optical strips*. These are directed to the lateral geniculate bodies, continuing with the optical radiation to the medial region of the occipital lobe.

The sudden presentation of visual deficit points towards ischaemic, demyelinating or traumatic aetiologies, while progressive deficit is characteristic of the infiltrative or compressive processes.

Lesions of the intraorbital segment of the optic nerve cause a central scotoma.

Non-arteritic anterior ischaemic optic neuropathy (NAION) is the most common cause of unilateral vision loss and papilloedema (papillitis) in adult individuals (older than 50 years) with cardiovascular risk factors, while in older patients NAION is caused by giant cell arteritis.

Optic neuritis is inflammation of the optic nerve secondary to demyelination. Typically, it affects adults between 20 and 50 years old (more common in women). It is rare in children.[14] Diagnosis is clinical. MRI can show thickening of the optic nerve and signal hyperintensity in T2 and post-contrast enhancement, indistinguishable from other inflammatory processes. The presence of lesions in cerebral

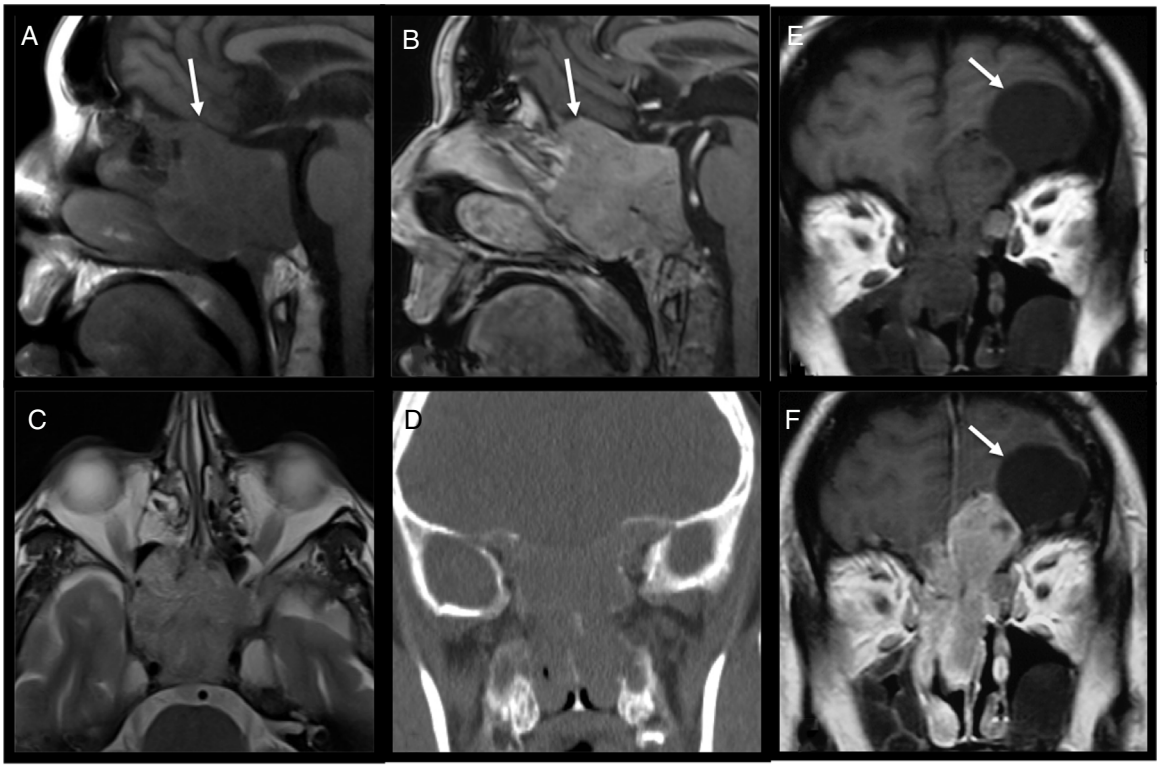

Figure 3 Esthesioneuroblastoma. A large mass is observed centred on the posterior region of the nasal passages that infiltrates the ethmoid, sphenoid and clivus and shows extension towards the anterior cranial fossa (arrow). (A) In the sequence enhanced in T1, it presents intermediate signal intensity characteristic of this type of tumour. (B) Sagittal enhanced in T1 post-contrast that shows homogeneous enhancement with intravenous contrast. (C) In the axial sequence enhanced in T2, the tumour also presents an intermediate signal as in T1. (D) The tomographic image shows the important bone destruction of the base of the skull. (E and F) Coronal images enhanced in T1, without contrast (E) and with contrast (F), from another patient, in which esthesioneuroblastoma is observed with intracranial invasion and non-neoplastic cyst in the interface (arrow).

white matter in MRI is the most important predictor for the development of multiple sclerosis; therefore, in the face of an episode of optic neuritis, the MRI study is mainly aimed at detecting demyelinating encephalic lesions.

The remaining causes that produce optic neuropathy can be seen in Table 4 (Fig. 4).

In *the orbital apex*, the defect is usually sectoral.

The compression of the body of the *chiasm* produces a bitemporal hemianopsia, more commonly produced by pituitary tumours.

Post-chiasmatic lesions lead to congruent homonymous deficits, which means identical defects in each eye, and respect the macula.

Semiology and pathology of cranial nerves III–XII

The isolated involvement of the cranial nerves can be associated with specific clinical signs and symptoms (Table 2). The complex lesions that associate paralysis of several pairs are due to meningeal pathology, of the trunk and of the base of the skull. The lesions in the trunk associate motor and sensory deficits.

The pathology of the cranial nerves, according to the affected anatomical segment, can be seen in Table 5.

Although there are peculiarities of each cranial pair, cranial nerves III–XII share some pathological processes:

- *Glioma of the trunk* is more common in children and in the pons. It is usually a low-grade diffuse glioma. In MRI, the characteristic image is an infiltrative lesion, expansive, heterogeneous in T2 and hypointense in T1 with variable enhancement. It frequently produces paralysis of nerves VI and VII, ataxia and signs of involvement of long tracts.
- In adults, the tumours that most frequently affect the trunk are metastases, especially lung and breast metastases, and lymphoma.
- *Trunk syndromes* are usually of ischaemic origin. They combine motor and sensory deficits with cranial nerve palsy (Table 6).
- In MRI, the *infectious involvement of the trunk* is manifested by increase of volume, signal hyperintensity in T2 and enhancement (Table 2).
- *Meningeal involvement with involvement of the cisternal segment* by inflammatory and tumour processes, such as meningeal carcinomatosis and lymphoma, often results in deficits of multiple cranial nerves that are usually progressive. The MRI shows enhancement and thickening of the cisternal segments of the nerves, and meningeal enhancements, and often it is the 3D-FLAIR post-contrast sequence that is the most sensitive for its detection.[6]

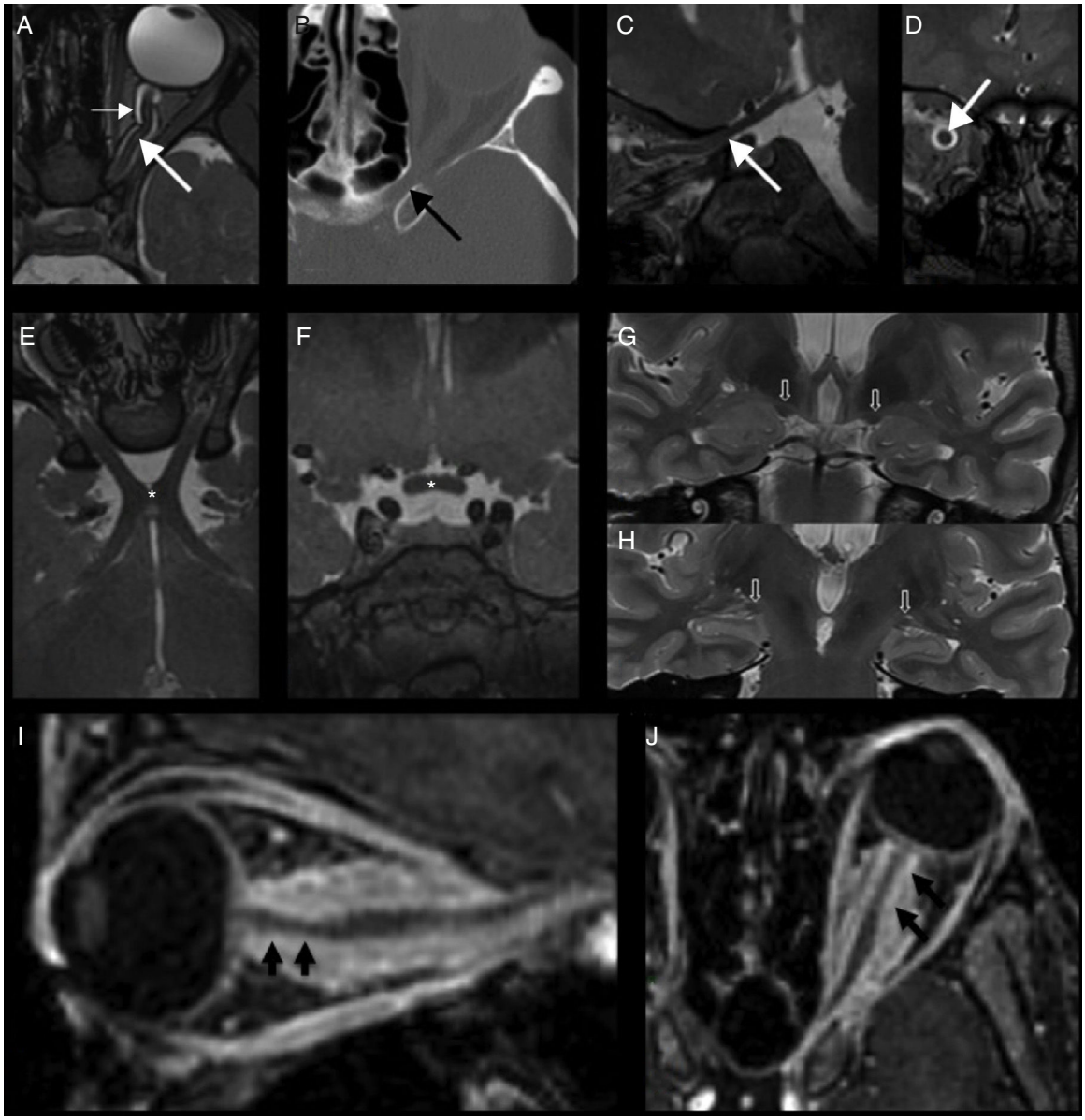

Figure 4 Anatomy and meningioma of the optic nerve sheath. (A–D) Trajectory of the optic nerve in the orbit and optic canal (thick white arrow), with its sheath (thin arrow) in T2-weighted sequences; bone walls of the optic canal in tomographic examination (black arrow). Images (E) and (F) show the optic chiasm in axial and coronal planes, respectively. Visualisation of the optical strips (hollow arrows) in two successive coronal sections (G and H). Sagittal (I) and axial (J) slices of T1-weighted sequences with post-contrast fat suppression, showing the characteristic magnetic resonance image of the optic nerve meningioma in ''tram tracks'' referring to the concentric thickening and enhancement of the optic nerve sheath. There is a slight narrowing of the optic nerve in its proximal portion (arrows).

They usually manifest with involvement of VII, III, VI and lower cranial nerves IX, X and XI. In the differentiation of inflammatory and tumour involvement, clinical correlation and laboratory tests, especially the CSF analysis, will be essential (Fig. 5).

- *Schwannoma or neurinoma* is the most common primary neoplasm of the cranial nerves. It originates in the myelin sheath of the cranial nerves, most often in the sensory nerves. When it occurs in mixed or motor nerves, type 2 neurofibromatosis or schwannomatosis is usually associated and it affects multiple nerves. The most common location is the lower division of the VIII pair, followed by the V, X, XII and VII.[15] In the VIII pair they appear as intracanalicular and cistern masses with characteristic morphology of an ice-cream cone. Less frequently they are exclusively intracanalicular, extracanalicular or labyrinthine (Fig. 6).
- *Neurofibromas* can originate from Schwann cells, from other perineurial cells or from fibroblasts. They are more common outside the skull and are associated with type

Table 4 Pathology of the visual pathway.

Pathology	Prechiasmal	Chiasmal	Retrochiasmal
Congenital	Coloboma Leber's hereditary optic neuropathy Septo-optic dysplasia		
Traumatic	Section or compression of the optic nerve by bone fragment or foreign body Avulsion Indirect injury: oedema, ischaemia		Brain contusion Brain haemorrhage
Vascular	Carotid-cavernous fistula Ischaemia		Ischaemia Haemorrhage Vascular malformation
Degenerative	Drusen		
Inflammatory	Optic neuritis Neuromyelitis optica Sarcoidosis Systemic lupus erythematosus Inflammatory pseudotumour Infections Graves' disease Optic perineuritis	Sarcoidosis Tuberculosis Optic neuritis	Sarcoidosis Tuberculosis Optic neuritis
Primary neoplasms	Optic nerve glioma Perioptic meningioma Lymphoproliferative disorders	Optic nerve glioma Perioptic meningioma Lymphoproliferative disorders	Brain glioma Brain lymphoma
Extrinsic neoplasms	Lymphangioma Epidermoid cyst Dermoid cyst Meningioma Myeloma	Macroadenoma Craniopharyngioma Meningioma Hemangiopericytoma Chondrosarcoma	Meningioma Metastasis
Secondary neoplasms	Metastasis (extrinsic compression)	Metastasis (extrinsic compression)	Metastasis
Other causes of extrinsic compression	Fibrous dysplasia Nasosinusal pathology (mucocele, subperiosteal abscesses, neoplasia)	Arachnoid cyst Rathke's cyst	
Other	Idiopathic intracranial hypertension		

1 neurofibromatosis. In the image they are well defined, they can contain calcification and they enhance moderately. Haemorrhage and cysts are less common.[15]

- *Paragangliomas* are neuroendocrine tumours that are derived from the chromaffin cells of the extrarenal paraganglionic system. They usually establish themselves in four different locations: in the carotid bifurcation, accompanying the vagal nerve, in the jugular foramen and in the middle ear. They are usually familiar and multicentric. The most common are the carotid and jugular paragangliomas. Although usually benign, paragangliomas can malignify in 3–4% of cases.[16]

In the jugular foramen, they affect the lower cranial nerves and manifest as solid tumours with lobulated or oval morphology. Occasionally, they may extend to the middle ear (jugulotympanic paraganglioma) (Fig. 7). Carotid and vagal paragangliomas have the same characteristics in MRI, although they do not destroy the bone, as they are far from it. The different displacement they produce from the internal and external carotids is used to differentiate them (Fig. 8).

Ophthalmoplegia and diplopia

Binocular diplopia is the main symptom caused by lesion or pathology of nerves III, IV and VI, which supply the extraocular muscles (Table 2).

Involvement of the intra-axial segment

Ischaemia occurs more frequently in the pons. At this level, infarcts do not cross the midline and follow the distribution of the perforating branches of the basilar artery. In the

Table 5 Pathology of cranial nerves III–XII.

Pathology	Intra-axial segment	Cisternal segment	Dural and interdural segments Meckel's *Cave* and cavernous sinus (III, IV, VI, V1, V2)	Foraminal segment and base of skull
Congenital	Aplasia or hypoplasia of the nerve and nuclei	Aplasia or hypoplasia Arachnoid cyst		
Traumatic	Haemorrhage	Section		Compression or section due to bone fracture of the base of the skull, orbit and face
Vascular	Infarction Haemorrhage Cavernoma Arteriovenous malformation	Ischaemia Vascular compression by arterial or venous loop Compression by vascular malformation Subarachnoid haemorrhage	Carotid aneurysm Carotid-cavernous fistula Thrombosis of the cavernous sinus	Arteriovenous malformation
Inflammatory and infectious	Demyelinating disease Bickerstaff's encephalitis Miller-Fisher syndrome Systemic lupus erythematosus Acute disseminated encephalomyelitis PML Herpes zoster HIV encephalitis Behçet's disease Lyme disease Whipple's disease Listeria encephalitis	Multiple sclerosis Chronic inflammatory demyelinating polyneuropathy Sarcoidosis Tuberculosis Disease related to IgG_4 Fungal infection Meningitis Herpes simplex and varicella zoster Idiopathic neuropathy Fisher's syndrome	Aggressive bacterial and fungal sinusitis Sarcoidosis Wegener's granulomatosis Tolosa-Hunt syndrome	Aggressive bacterial or fungal infection Petrositis: Gradenigo's syndrome (V, VI, VII, VIII) Wegener's granulomatosis Osteomyelitis due to infection of the paranasal sinuses Cholesteatoma (VII)
Neoplasms	Glioma lymphoma	Schwannoma Neurofibroma Lipoma	Schwannoma Meningioma Malignant Schwannoma Hemangiopericytoma Pituitary adenoma Chordoma and chondrosarcoma of the base of the skull Lymphoma	Schwannoma Paraganglioma (jugular foramen) Meningioma Plexiform neurofibroma Clival chordoma Myeloma
Secondary neoplasms	Metastasis	Perineural dissemination Meningeal carcinomatosis Secondary lymphoma	Metastasis Perineural dissemination	Perineural dissemination Haematogenous metastases (lung, prostate, breast) Tumour invasion (squamous cell nasopharyngeal carcinoma)
Other causes of extrinsic compression	Fibrous dysplasia Nasosinusal pathology (mucocele, subperiosteal abscesses, neoplasia)	Meningioma Schwannoma Epidermoid cyst Lipoma Tumours of the base of the skull (chordoma, sarcomas, metastasis, etc.) Large tumours of the cerebellopontine angle Tumours of the nasopharynx, paranasal sinuses, etc.	Pituitary apoplexy Extension of orbital pathology	Non-neoplastic bone lesions: • Paget's disease • Histiocytosis • Fibrous dysplasia

PML:

Table 6 Trunk syndromes.

Syndrome	Location of the lesion	Cranial nerve involved	Other deficits
Weber's syndrome	Ventral midbrain region due to involvement of the corticospinal and corticobulbar pathways of the cerebral peduncle	Fascicle of the III nerve Ipsilateral III nerve	Contralateral hemiplegia or hemiparesis
Benedikt syndrome	Midbrain Red nucleus	Nucleus of the III nerve Ipsilateral III nerve	Hemiataxia and contralateral choreoathetosis
Claude syndrome	Dorsomedial region of the midbrain with involvement of the medial region of the red nucleus, the rubrodentate fibres and the superior cerebellar peduncle	Nucleus of the III nerve Ipsilateral paralysis of the III nerve	Contralateral arm and leg ataxia
Nothnagel syndrome	Quadrigeminal plate and superior cerebellar peduncle	Nucleus of the III nerve Ipsilateral paralysis of the III nerve	Leg ataxia
Lateral pontine syndrome or Marie–Foix or Marie–Foix–Alajouanine syndrome	Lateral infarction of the pons Involvement of the corticospinal tract Cerebellar tracts	Nuclei of nerves VII and VIII Facial paralysis Sensorineural hearing loss, ipsilateral vertigo and nystagmus	Contralateral hemiplegia or hemiparesis Ataxia of ipsilateral extremities
Inferior medial pontine or Foville syndrome	Involvement of the corticospinal tract, the medial lemniscus and the middle cerebellar peduncle	Nuclei of nerves VI and VII Facial paralysis, diplopia and ipsilateral horizontal gaze paralysis	Contralateral hemiplegia or hemiparesis Loss of proprioception and contralateral vibration
Captivity syndrome	Involvement of the pyramidal pathway. The midbrain preserved with III nerve intact. Preserved consciousness and cognition with paralysis of all voluntary muscles	Paralysis of nerves VI and VII	Tetraparesis Respiratory failure
Raymond syndrome	Lesion of the ventral pons Corticospinal fibres Corticofacial fibres	Ipsilateral fascicle of the VI nerve Horizontal conjugate gaze palsy	Contralateral hemiparesis Facial paresis
Millard-Gubler syndrome	Lesion of the ventral pons Pyramidal tract	Nuclei of VI and VII Ipsilateral facial paralysis, absence of corneal reflex and diplopia and exotropia	Contralateral hemiplegia
Facial tubercle syndrome	Medial longitudinal fasciculus	Nucleus of the VI nerve and knee of the VII nerve Decreased taste in front two thirds of the tongue, hyperacusis, diplopia	Horizontal conjugate gaze palsy
Wallenberg syndrome	Lateral bulbar syndrome Inferior cerebellar peduncle	Nucleus of the VIII vestibular symptoms Spinal nucleus of V nerve with acute pain in the face ipsilateral Ambiguous nucleus: dysphonia, dysphagia, dysarthria and decreased gag reflex	Ipsilateral ataxia Hypoalgesia and temperature in the contralateral hemibody
Dejerine syndrome	Medial bulbar syndrome	Ipsilateral paralysis of the XII nerve	Contralateral hemiplegia or hemiparesis and hemianesthesia Nausea, vertigo and contralateral ataxia
Babinski–Nageotte syndrome	Hemibulbar syndrome		Contralateral hemiplegia

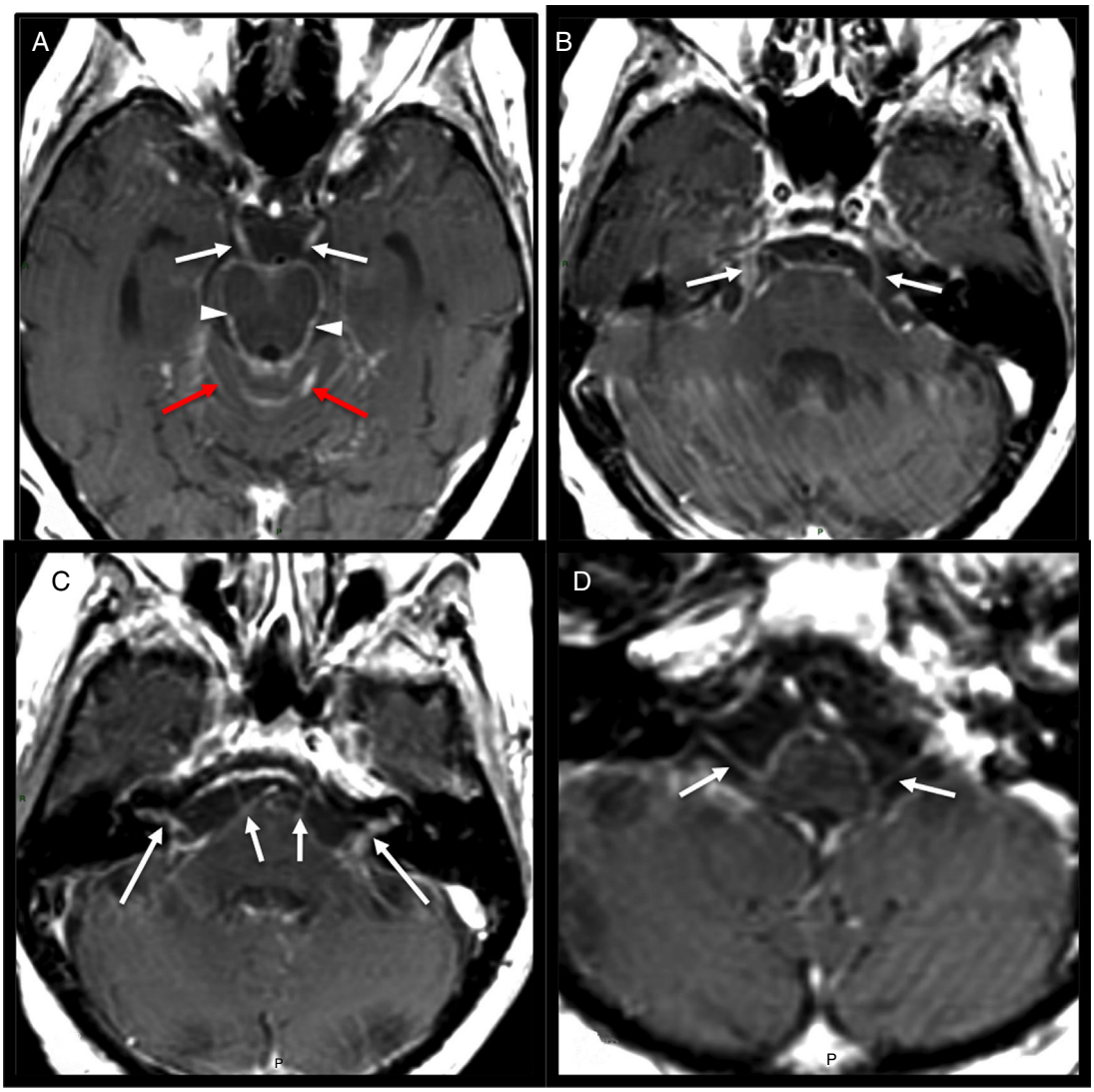

Figure 5 Meningeal carcinomatosis. A 62-year-old woman with a history of breast carcinoma with multiple cranial nerve palsies. Axial slices of FSE sequence enhanced in T1 post-contrast. (A) Leptomeningeal enhancement in the basal cisterns (arrowheads) and in the cerebellar folia (red arrows), as well as the III nerve on both sides (white arrows). (B) Of the trigeminal nerves (arrows). (C) Of the VI nerve pair bilaterally (short arrows) and of the VII and VIII cranial nerves in both inner auditory canals (long arrows). (D) of the lower nerves IX, X and XI (arrows).

midbrain, however, they can cross the midline and produce a more complex oculomotor symptomatology (Table 6).

Wernicke encephalopathy is a serious clinical picture caused by thiamine deficiency. It is characterised by ophthalmoplegia, ataxia and encephalopathy. It is reversible if intravenous vitamin B_1 therapy is started early.

Miller-Fisher syndrome is the most common form of non-classical variants of Guillain–Barré syndrome; it is characterised by partial or complete ophthalmoplegia, sensory ataxia, and areflexia. While MRI may show enhancement of cranial nerves, it is not necessary to perform it for diagnosis.[17]

Involvement of the cisternal segment

The most common causes of third nerve palsy in adults are ischaemia, the mass effect due to aneurysm, uncal herniation and tumours.

The microvascular involvement of the *III cranial nerve* may be responsible for its paralysis, or isolated paresis, in up to 75% of cases in individuals older than 45 years-old with cardiovascular risk factors. Less frequently, it is also a cause of isolated paresis of nerves IV and VI in adults.[18–20]

The extrinsic compression of the III cranial nerve usually produces non-reactive mydriasis. In these cases, it is necessary to rule out an aneurysm in the posterior communicating artery, and, to a lesser extent, in the tip of the basilar artery. However, in patients younger than 45 years-old, even without pupillary involvement, a compressive cause should be ruled out. The expansive processes of the cerebral hemispheres that cause transtentorial herniation can produce paralysis or paresis isolated from the III and VI nerves.

The trochlear nerve, however, is the most vulnerable to head injuries.[19]

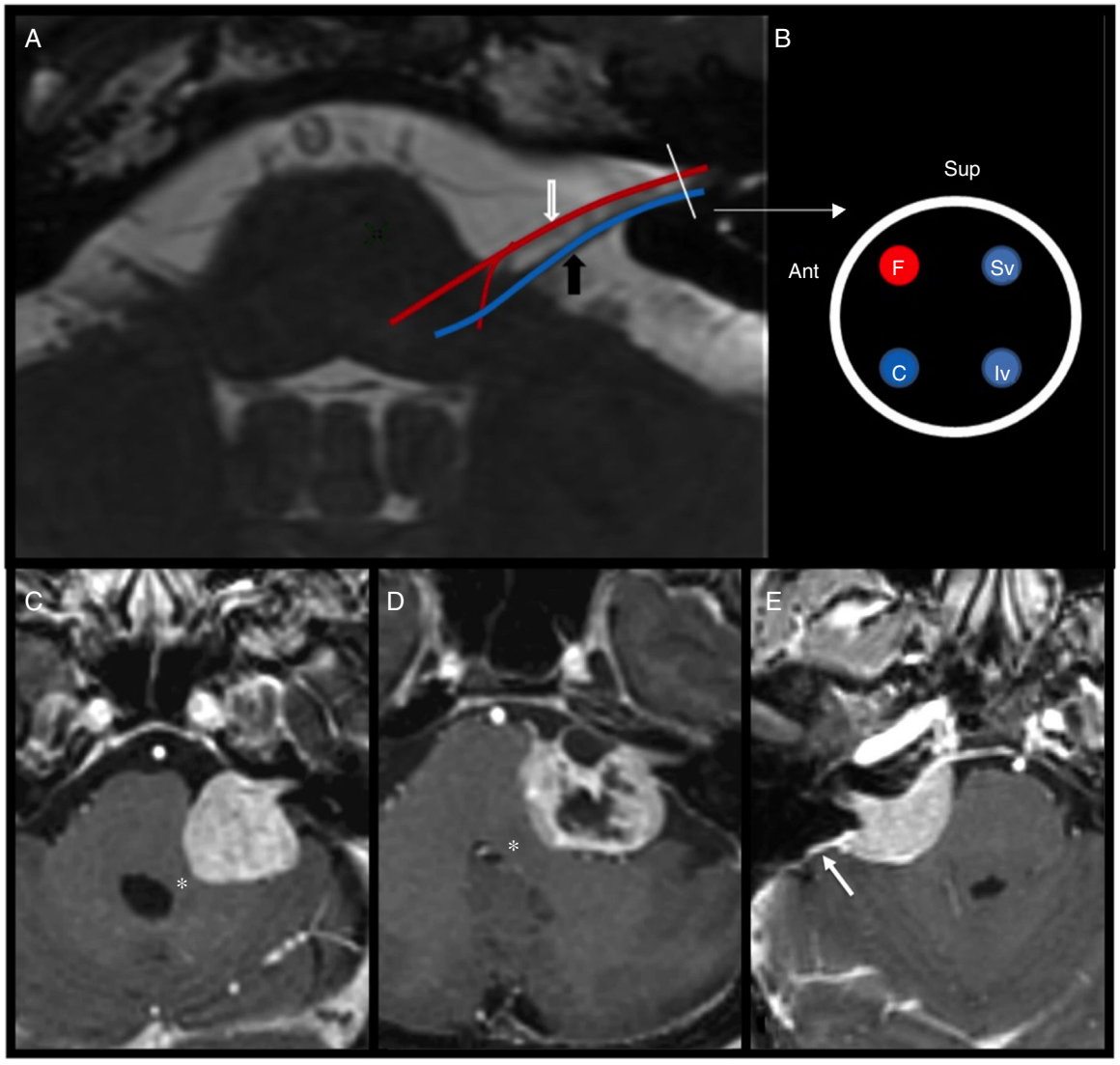

Figure 6 Anatomy and injuries of the VIII nerve. (A) Axial section at the level of the pons, showing the fascicular and cisternal path of the VII nerve (white arrow) and VIII nerve at the cerebellopontine angle (black arrow). (B) Relative position of the facial (F), cochlear (C), superior vestibular (Sv) and inferior vestibular (Iv) nerves at the vertex of the internal auditory canal. (C and D) Axial slices of post-contrast T1-weighted sequences show the corresponding acoustic neurinomas. Both show the typical ice-cream cone morphology of these tumours, with intracanalicular and cisternal component, and cystic component with absence of enhancement in D, also common in these tumours. In both cases, the tumour compresses the adjacent middle cerebellar peduncle (asterisk). (E) Axial section of T1-weighted post-contrast sequence showing a tumour with homogenous enhancement in the cerebellopontine angle cistern and extension to the interior of the internal auditory canal corresponding to a meningioma. The broad base of implantation and dural tail (arrow) can be observed, findings that make it possible to differentiate it from schwannoma.

The involvement of primary tumours such as schwannoma is rare, and is more common in neurofibromatosis type 2 and in schwannomatosis. Compression is more common due to extra-axial tumours (epidermoid cysts) and secondary involvement (meningeal carcinomatosis, leukaemic or lymphomatous infiltration). Clivus tumours such as meningiomas, metastases, and bone tumours such as chordoma often affect the VI nerve (Figs. 5, 9 and 10).[21]

In childhood, *ophthalmoplegic migraine* (considered an idiopathic inflammatory cranial mononeuropathy) presents with recurrent headaches and paresis of one or more oculomotor nerves (Fig. 9).[22]

Lesions of the cavernous sinus can produce ophthalmoplegia (III, IV, and VI), anisocoria or mydriasis (III), and deficits of V1 and V2, chemosis, proptosis, and Horner syndrome due to involvement of the oculosympathetic fibres around the internal carotid artery (Fig. 11 and Table 3).

Lesions in the superior orbital fissure or sphenoid cleft lead to the involvement of III, IV, VI and V1 nerves and of the superior ophthalmic vein with ophthalmoplegia, V1 neuropathy, proptosis, chemosis and fixed mydriasis.

Tolosa-Hunt syndrome, self-limiting and recurrent painful ophthalmoplegia, produced by a granulomatous inflammation of the cavernous sinus or superior orbital

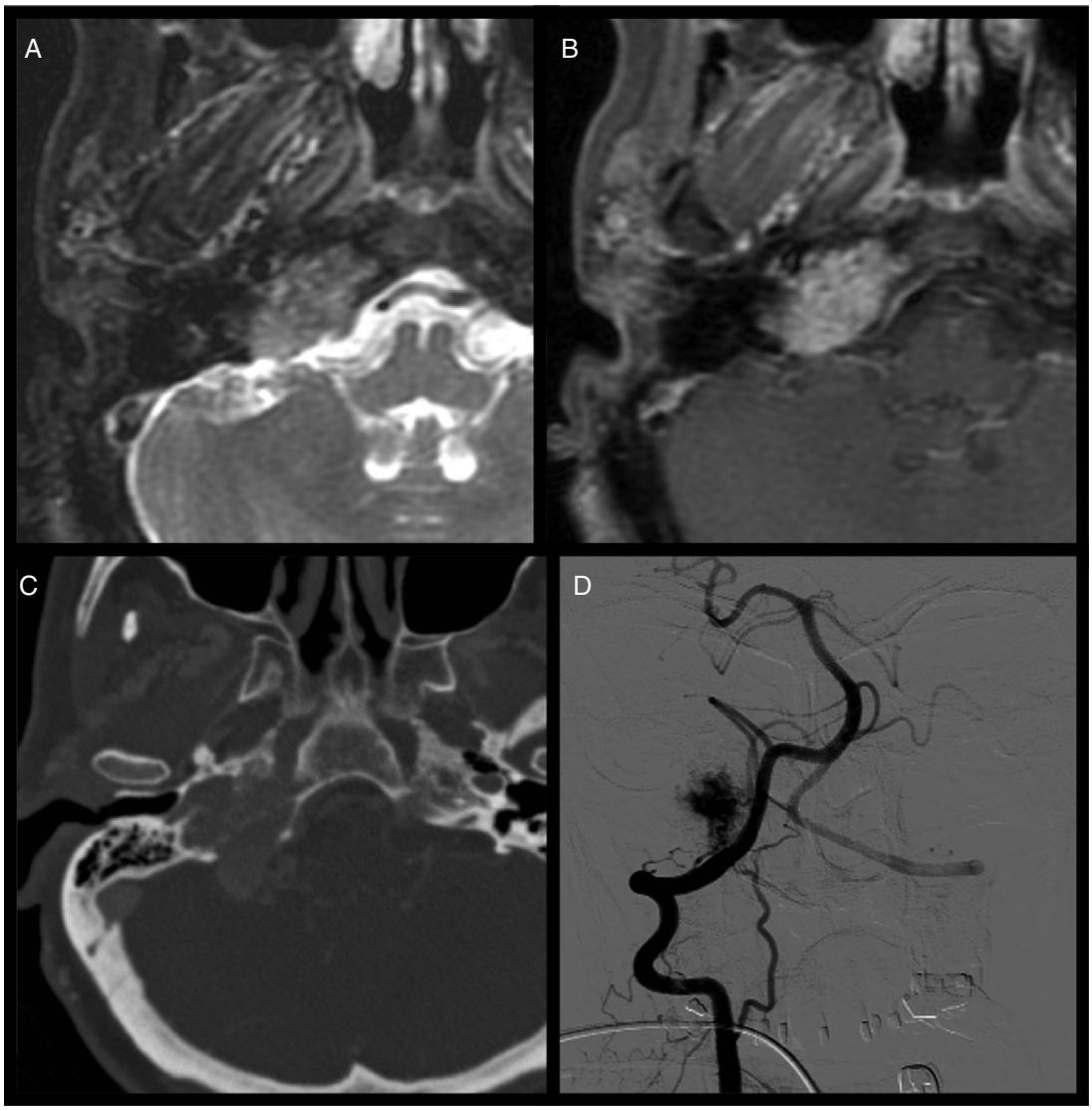

Figure 7 Jugular paraganglioma. (A) FSE axial sequence enhanced in T2, showing a heterogeneous signal intensity tumour, irregular contour in the jugular foramen, compatible with jugular paraganglioma. In the case of large lesions, there may be the characteristic ''salt and pepper'' appearance, with hyperintense foci in T1 that represent areas of subacute haemorrhage, and hypointense foci in T2 that reflect signal emptiness in high-flow vessels. (B) The lesion intensely enhances post-contrast. (C) Computed tomography shows bone destruction in the jugular foramen, unlike what occurs in schwannomas or meningiomas, in which bone remodelling and sclerosis occur, respectively. (D) The digital angiography performed for preoperative embolisation confirms the hypervascular nature of the lesion, with marked repletion in the early arterial phase from occipitocervical perforating branches of segment V3 of the right vertebral artery.

fissure, is a diagnosis of exclusion. In the differential diagnosis, meningioma and lymphoma must be included.

Trigeminal neuropathy

Trigeminal neuropathy produces anaesthesia, pain or burning in the regions supplied by each branch (Table 2). MRI is essential for diagnosis.

Involvement of the *nuclear or fascicular segment* may be the first presenting symptom of multiple sclerosis.

The *involvement of the cisternal segment* can be manifested with paresis, sensory symptoms and decreased corneal reflex. The most common pathologies are tumours, infections and vascular compression (Table 5) (Figs. 5, 10 and 12). It can also manifest with neuralgia, most frequently in the territory of V2 and V3. In individuals older than 40 years-old, it is usually idiopathic, although vascular compression is sometimes demonstrated. The most vulnerable nerve portion corresponds to the transition zone. The arteries most commonly involved are the superior cerebellar artery and the anterior inferior cerebellar artery; venous compression is less common. The presence of atrophy or distortion and displacement of the nerve will support the diagnosis of neurovascular compression.[23] Some authors propose performing a DTI

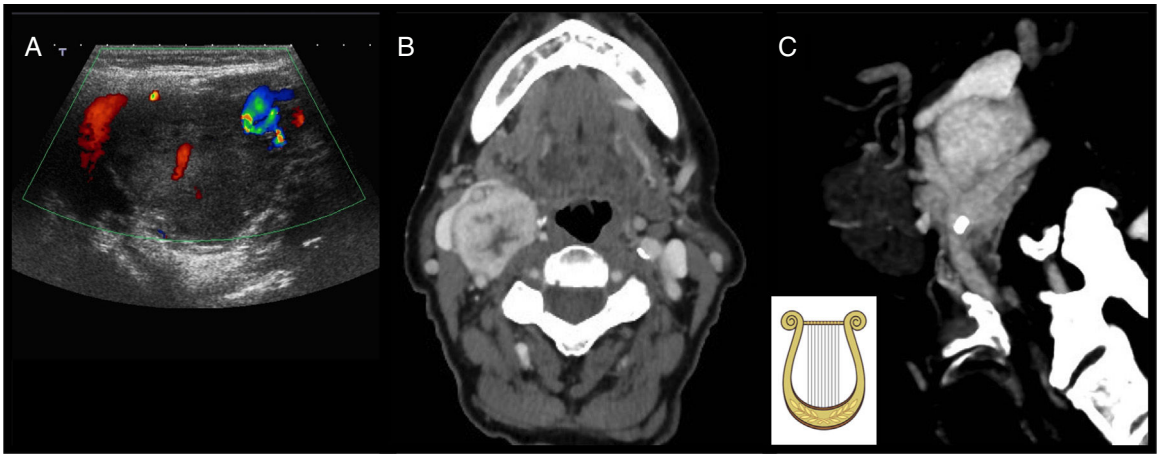

Figure 8 Carotid paraganglioma. (A) Echo-Doppler showing a solid tumour that separates the carotid bifurcation. (B) The post-contrast computed tomography image shows intense heterogeneous enhancement of the mass at the carotid bifurcation. (C) In the reformatted parasagittal image we see the lesion in the bifurcation separating both carotids (lyre sign), while the vagal paraganglioma displaces them anteromedially.

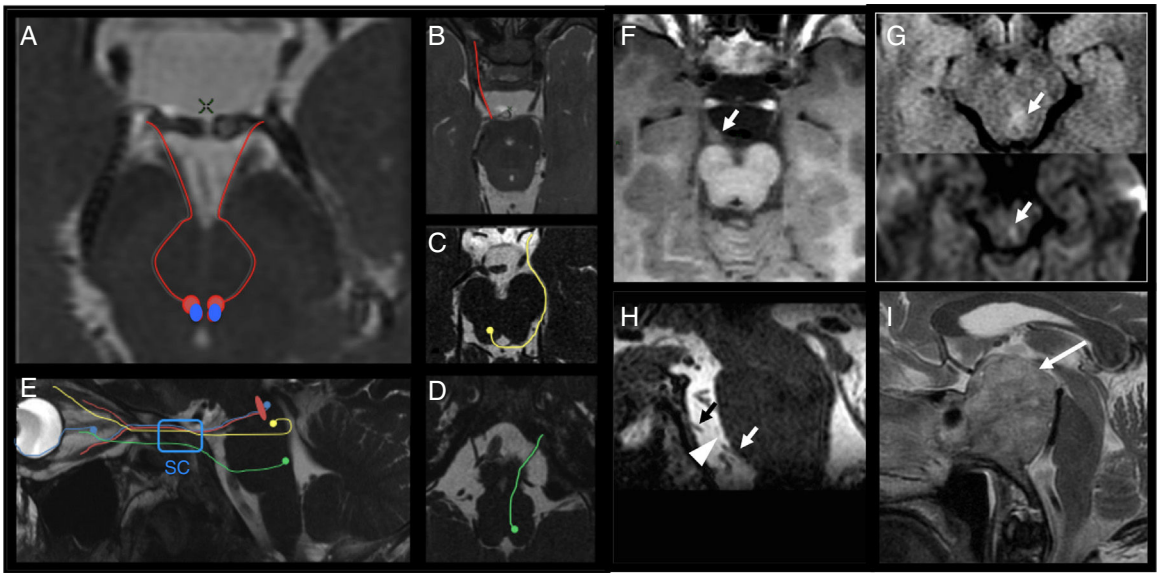

Figure 9 Anatomy and isolated paralysis of oculomotor nerves. (A) Mesencephalic location of oculomotor (red) and Edinger–Westphal (blue) nuclei of the III cranial nerve, showing its fascicular and cisternal path (red) in oblique axial plane. (B) Cisternal path of the III cranial nerve. (C) Nucleus and path of the cisternal portion of the IV nerve (yellow), with emergence from the dorsal contralateral portion of the midbrain. (D) Nucleus and cisternal path of the VI nerve (green) in oblique section at the level of the pons until its entrance into the Dorello canal. (E) Sagittal reconstruction of the 3D FIESTA sequence, showing the path of the three previously mentioned nerves, and the situation of the intracavernous segment (CS, blue box). (F) GR sequence enhanced in T1 showing thickening of the right III nerve at its origin (arrow) in a case of ophthalmoplegic migraine. The III nerve is the one that is affected most frequently. There also tends to be a post-contrast enhancement. (G) A small hyperintense lesion (arrow) is seen in the FLAIR sequence enhanced in T2 (upper) with diffusion restriction (lower) corresponding to an acute lacunar infarct in the nucleus of the IV nerve. (H) 3D FIESTA sequence in which a discontinuity (arrowhead) can be seen in the middle third of the VI nerve (white and black arrows) secondary to rupture due to traumatic brain injury. (I) Sagittal T2 showing a tumour infiltrating the clivus, corresponding to a chordoma with a large extraosseous component (arrow) that compresses the pons and the cisternal path of the VI nerve.

sequence which demonstrates a decrease of the values of fractional anisotropy in the affected nerve.[9]

The *cavernous sinus and the orbital apex* are common sites of perineural dissemination of some neurotropic tumours, such as adenoid cystic, mucoepidermoid and squamous cell carcinomas, melanoma and lymphoma. As in the lesions of the superior orbital fissure, the involvement is usually limited to V1. The MRI showed thickening and enhancement of the affected nerve and signs of secondary denervation.

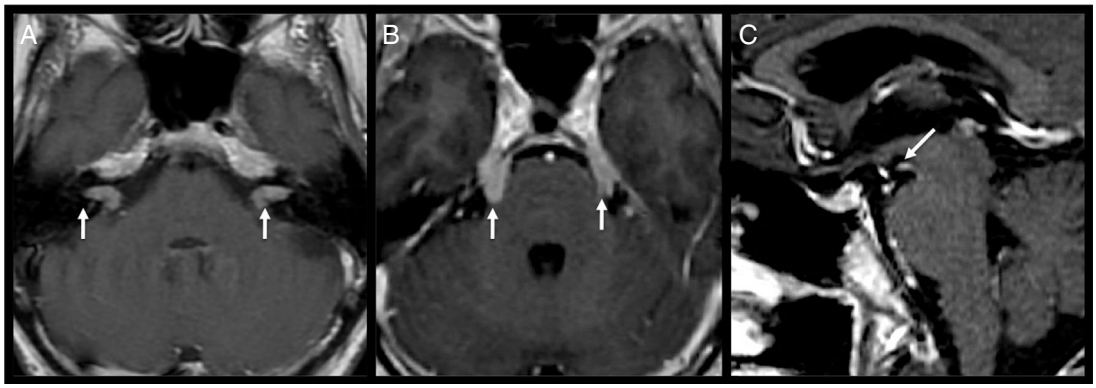

Figure 10 Secondary leptomeningeal dissemination of lymphoma. A 54-year-old male with a history of non-Hodgkin's lymphoma who consulted due to left facial paralysis, central vertigo and right hearing loss. (A) Axial section of FSE sequence enhanced in T1 in which nodular enhancements are observed in both internal auditory canals simulating acoustic neurinomas (arrows). Images reformatted in axial (B) and sagittal (C) 3D GR sequence enhanced in T1. Image B shows the enhancement of both trigeminal nerves (arrows) and image C shows nodular enhancement in the apparent origin of the left third pair (arrow).

Petrous apex syndrome or *Gradenigo's syndrome* consists of paralysis of the VI nerve with hypesthesia and pain in the territory of V1. Divisions V2 and V3 may also be affected at times. Among the causes are suppurative otitis media or mastoiditis, neoplasms, traumatisms, inferior petrosal sinus thrombosis, etc.

Facial paralysis

Involvement of the facial nerve results in peripheral facial paralysis, while involvement of the supranuclear structures produces central facial paralysis.

Peripheral paralysis is idiopathic in 80% of cases (Bell's palsy). Imaging studies are indicated when there is a deficit of other cranial nerves, there is no clinical recovery after 3–6 weeks from the onset of symptoms or there are muscle spasms or contractions, which suggests a structural cause.

In the *cisternal segment*, facial paralysis is commonly attributed to tumoural causes: meningeal carcinomatosis, acoustic neurinomas, or more rarely of the facial nerve or lymphoma (Fig. 10).[24]

Involvement of the nerve in the *facial canal* is, most commonly, secondary to infections of the middle ear and especially to cholesteatomas (which present restriction to diffusion in the diffusion sequences), and less commonly to tumours such as schwannomas, hemangiomas, meningiomas, jugulotympanic paragangliomas and malignant bone tumours, especially chondrosarcoma (Fig. 13).

The presence of post-contrast enhancement in MRI of the intracanalicular or labyrinthine portions should always be considered anomalous, while the enhancement in the rest of the portions, including the genicular nerve, should not be interpreted as a pathological finding.

Traumatisms with fracture of the petrous can cause facial paralysis, especially in longitudinal fractures (the most common), which usually involve the geniculate ganglion fossa, where the facial canal is weakest.[24]

The presence of peripheral facial paralysis secondary to a *parotid lesion* should suggest a malignant neoplasm.

Hemifacial spasm

It is considered a neurovascular compression syndrome of the face, normally produced by the anterior inferior (AICA) and posterior inferior cerebellar arteries (PICA) and the vertebral arteries.[23]

Sensorineural hearing loss, tinnitus and/or vertigo

Audiovestibular symptoms, such as asymmetric hearing loss, sudden sensorineural hearing loss, tinnitus and vertigo, should make us suspect pathology of the VIII nerve.

Hearing loss must be sensorineural to be attributed to involvement of the VIII nerve. Imaging studies are indicated in young people, and in older people when it is clearly asymmetric or unilateral.

Tinnitus is the perception of sound without any external sound source. The majority are primary, without an identifiable cause.

Non-pulsatile tinnitus only requires imaging tests (MRI) when hearing loss, vertigo or headache is associated.[25,26] Pulsatile tinnitus can be secondary to an anomaly or vascular tumour.

The causality of some variants of normality in the production of tinnitus, such as the high jugular gulf[27–29] or the vascular loops in contact with the VIII nerve is unclear. While for some authors these vascular loops (e.g. AICA) are anatomical variants with no clinical correlation,[30–32] others have found a higher incidence of such loops in patients with pulsatile tinnitus.[33,34]

The most common structural lesion in the internal auditory canal (IAC) or cerebellopontine angle associated with hearing loss and tinnitus is vestibular schwannoma (acoustic neurinoma) (Fig. 6).

Prolonged *vertigo* of acute onset is due to a loss of vestibular function, which is usually unilateral. The clinical examination is fundamental in the distinction between central and peripheral lesion.

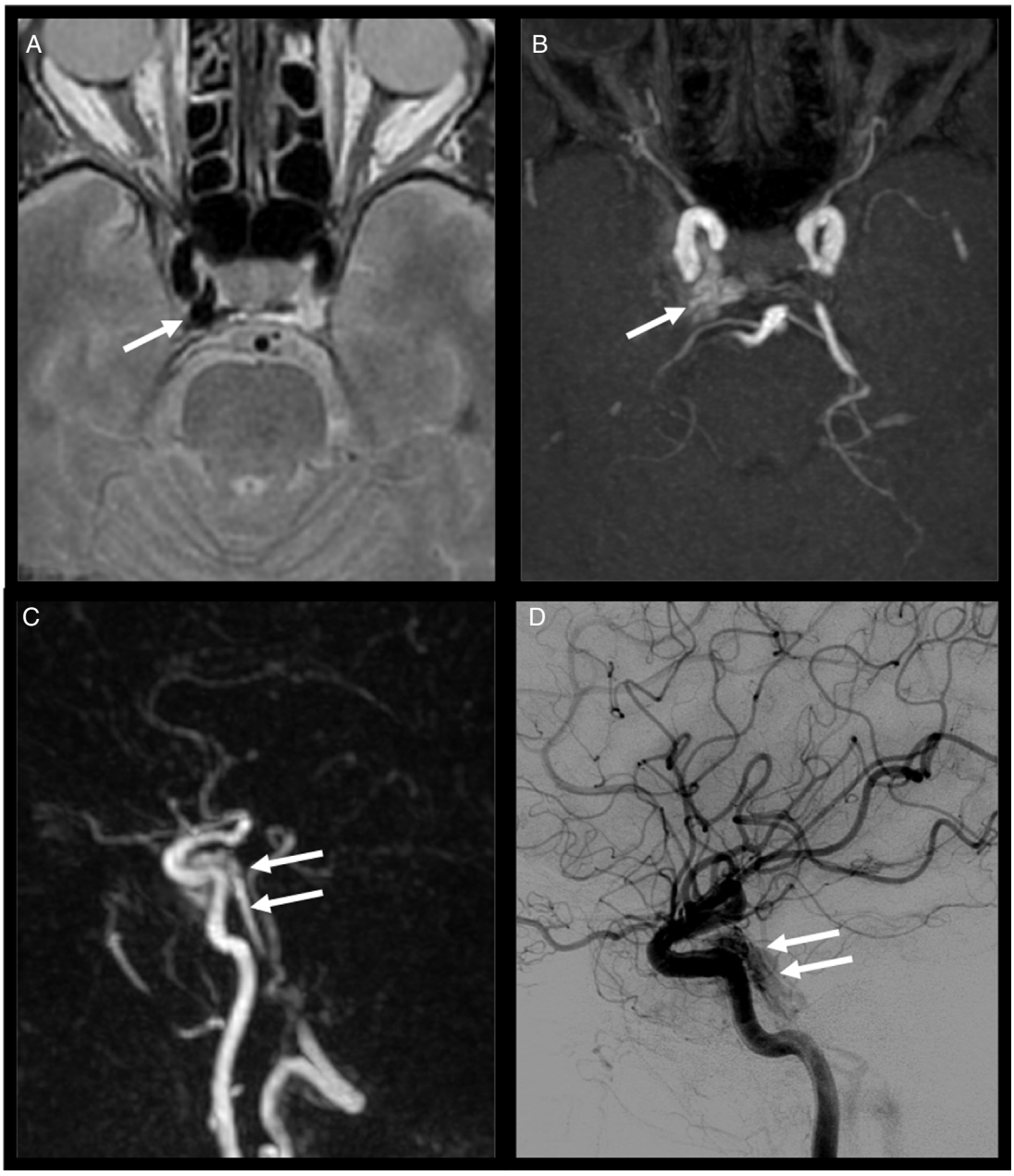

Figure 11 Carotid-cavernous fistula. A 59-year-old woman with a progressive picture of 3-month history of loss of visual acuity, conjunctival injection, palpebral oedema and right VI nerve palsy. (A) The PD-enhanced axial sequence shows an abnormal signal vacuum image inside the right cavernous sinus (arrow). (B) The 3D TOF sequence of the Willis polygon reveals arterialised flow signal in said location (arrow). (C) The sagittal reconstruction of the TRICKS sequence confirms the presence of contrast filling in the arterial phase of the cavernous sinus (arrows). (D) Angiography is performed for therapeutic purposes and reveals the same finding (arrows).

Vestibular paroxysm is considered a neurovascular compression syndrome of the VIII pair, most often caused by the anterior inferior and posterior inferior cerebellar arteries and the vertebral arteries.[23]

Lower cranial nerve neuropathy (IX, X, XI and XII)

The anatomical relationship of the lower cranial nerves IX, X and XI favours the joint complex neuropathy of all of them. Although the hypoglossal nerve (XII nerve) presents a different path at the base of the skull, its proximity means that it is also usually affected by the same pathologies, which is why it is included in this section.

In the cistern of the cerebellopontine angle, fusiform aneurysms of the vertebral artery and PICA, due to mass effect, can cause symptoms of lower nerves.

The remaining causes of involvement in the trunk and in the cisternal path are common to the rest of the cranial nerves (Table 3).

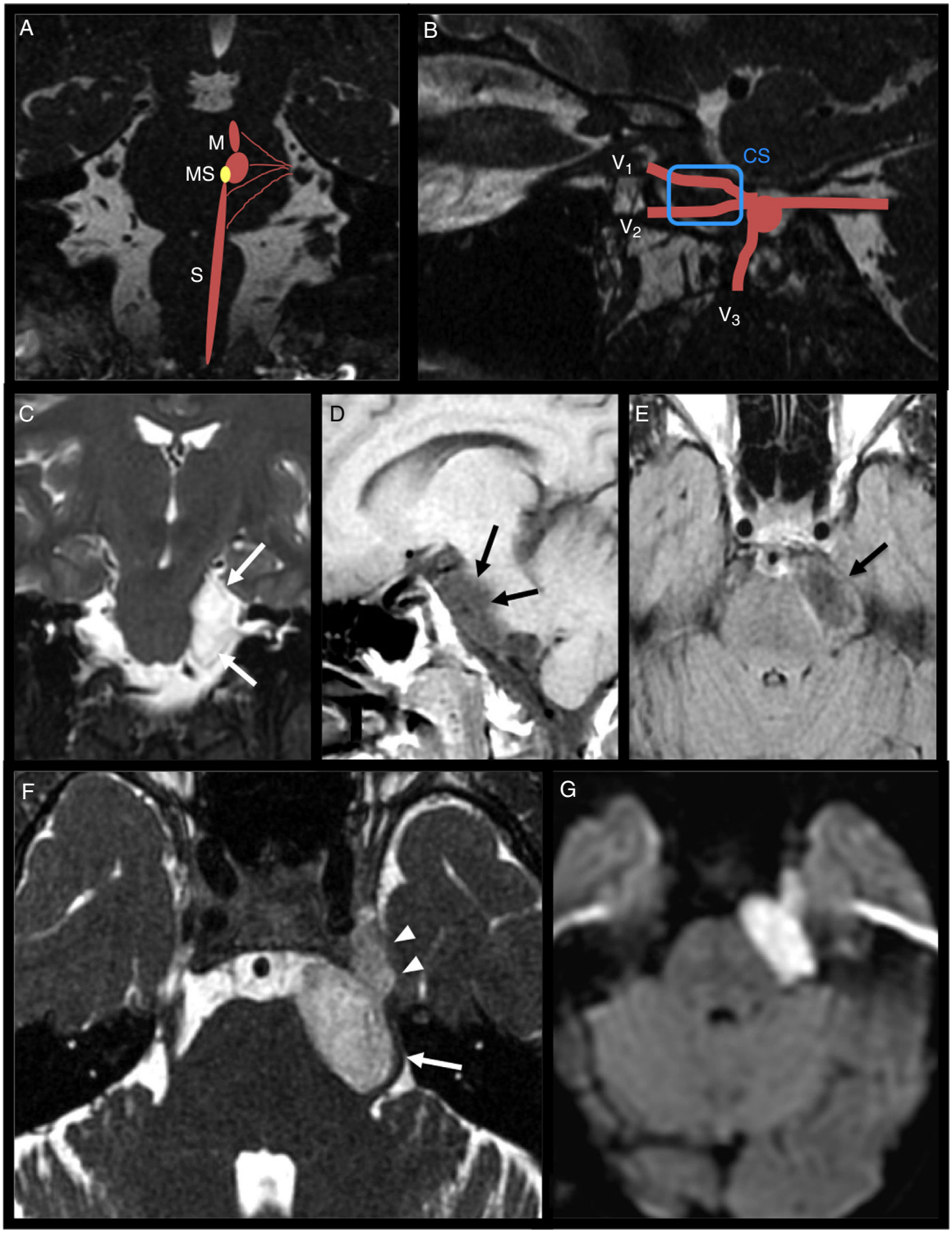

Figure 12 Anatomy of the V nerve. Epidermoid cyst. (A) Location of the mesencephalic (M), main somatic (MS) and spinal (S) nuclei of the V nerve, together with its motor nucleus (yellow), in an oblique coronal plane reconstruction of the 3D FIESTA sequence. (B) Sagittal reconstruction of the same sequence, showing the cisternal path of the V nerve up to its entrance to the Meckel's *cave*, location of the Gasser ganglion, and its three main branches V1, V2 and V3, together with the relative position of the first two in the interior of the cavernous sinus (CS, blue box). (C–G) Magnetic resonance images of a 36-year-old woman with left trigeminal neuralgia. The coronal image enhanced in T2 (C) shows a lesion in the cistern of the left cerebellopontine angle of signal intensity similar to cerebrospinal fluid (CSF), with slight mass effect on the pons (white arrows). (D) Sagittal T1 where the lesion presents a signal slightly higher than that of the CSF, as in (E) axial FLAIR enhanced in T2 (black arrows) showing hypointense signal of the lesion. (F) The FIESTA sequence confirms the signal difference of the lesion with respect to the CSF. It can be observed that the tumour externally displaces the cisternal segment of the V nerve (arrow) and enters the interior of the Meckel's *cave* (arrowheads). (G) The axial sequence enhanced in diffusion confirms the diagnosis of epidermoid cyst by revealing the restriction of diffusion.

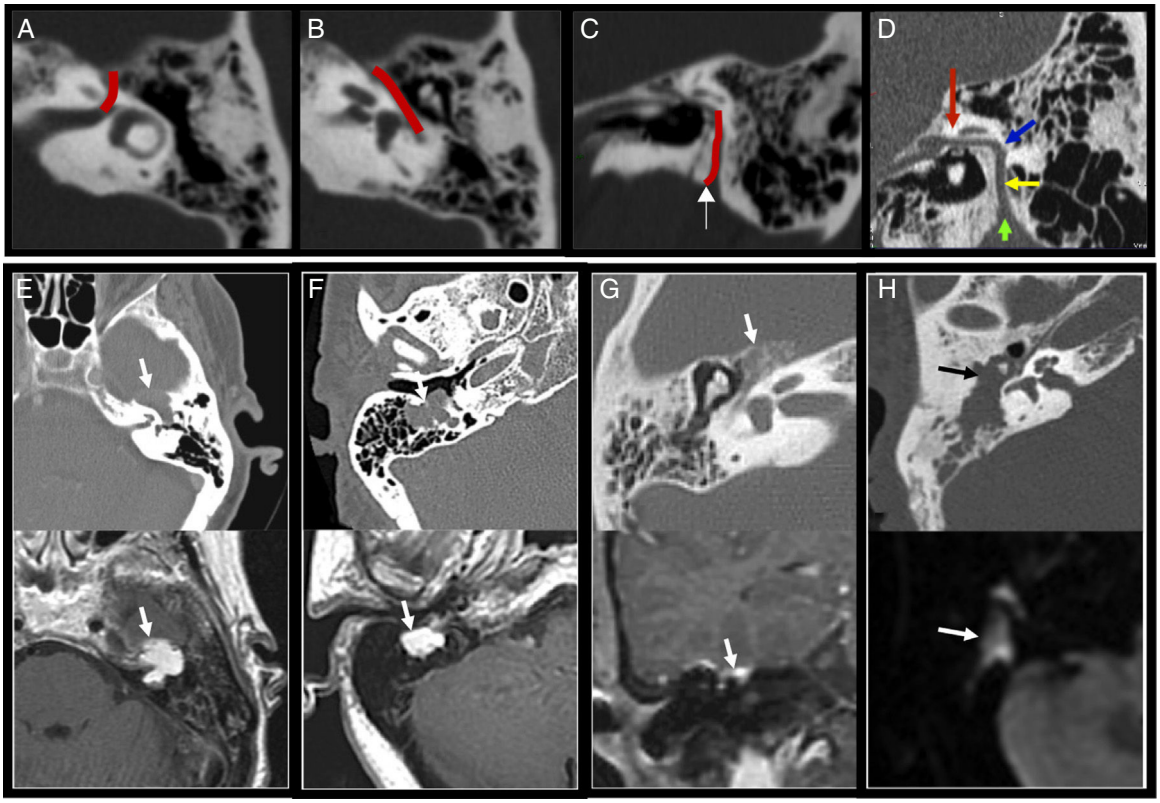

Figure 13 Anatomy and paralysis of the VII nerve. (A) Axial computed tomography (CT) section showing the labyrinthine segment. (B) Axial CT section showing the tympanic segment. (C) Coronal CT reconstruction showing the mastoid segment and the path of the facial nerve in the temporal bone until its exit through the stylomastoid foramen (arrow). (D) Coronal CT reconstruction showing the tympanic facial canal (red arrow), second knee (blue arrow), mastoid canal (yellow arrow) and stylomastoid foramen (green arrow). Four cases of patients with tumours in the intrapetrosal portion of the VII nerve are shown (Images E–H). (E) Schwannoma located in the region of the geniculate ganglion (arrows). (F) Schwannoma in the intramastoid vertical segment (arrow). Both lesions are presented on CT (upper images) as expansive lesions with well-defined borders, centred on the path of the facial nerve, and show intense homogenous enhancement after IV administration of gadolinium in T1 sequences (lower images). (G) The CT scan (upper image) shows a lytic lesion, although with a calcified honeycomb-shaped matrix characteristic of the haemangioma, that in T1 with post-contrast fat suppression (lower image) shows irregular enhancement. (H) The upper CT image shows a lesion occupying the eardrum, with partial ossicular destruction (black arrow) and in intimate contact with the tympanic portion of the facial nerve. The lower image shows diffusion restriction (arrow). Radiological findings characteristic of cholesteatoma.

At the base of the skull, they also share with the remaining cranial nerves the same causes of involvement of this segment, such as neoplasms (especially metastasis and chordoma), infections or trauma. The pathology that establishes itself in the jugular foramen causes simultaneous injury and combined neuropathy of nerves IX, X and XI, which is known as *Vernet's syndrome* or *jugular foramen syndrome*. It is usually caused by tumours, the most common being meningioma, schwannoma and paraganglioma; the latter more specific to this region (Fig. 7).

In the *suprahyoid neck*, the lower cranial nerves can be affected by carotid and vagal paragangliomas, schwannomas, malignant tumours, dissections and aneurysms of the internal carotid artery, and abscesses (Fig. 8).

The *isolated involvement of the glossopharyngeal nerve (IX nerve pair)* can manifest with sensory, motor and autonomic symptoms. Glossopharyngeal neuralgia may occur as a consequence of vascular compression, and may involve a branch of the PICA, the vertebral artery or a compression of the nerve between both.[23] Exceptionally, in its extracranial segment, entrapment of the nerve by an elongated styloid or by ossification of the stylohyoid ligament (Eagle's syndrome) may occur.

The *isolated involvement of the vagus nerve (X nerve pair)* usually occurs in the infrahyoid region of the neck, where only the vagus nerve continues to the mediastinum.

Isolated peripheral vagal neuropathy (recurrent laryngeal nerve) manifests with dysphonia secondary to paralysis of the ipsilateral laryngeal muscles (except the cricothyroid muscle), including the vocal cord. While on the left side, the recurrent laryngeal nerve turns around in the aortic arch and is affected with lesions of the latter (aneurysms) and mediastinal tumours or adenopathies, on the right side, said nerve ascends before, after surrounding the subclavian artery. Both can be injured by iatrogenesis, trauma or extralaryngeal neoplasm (especially oesophageal or pulmonary).

The involvement of the vagus nerve distal to the origin of the recurrent laryngeal nerve may be caused by thoracic

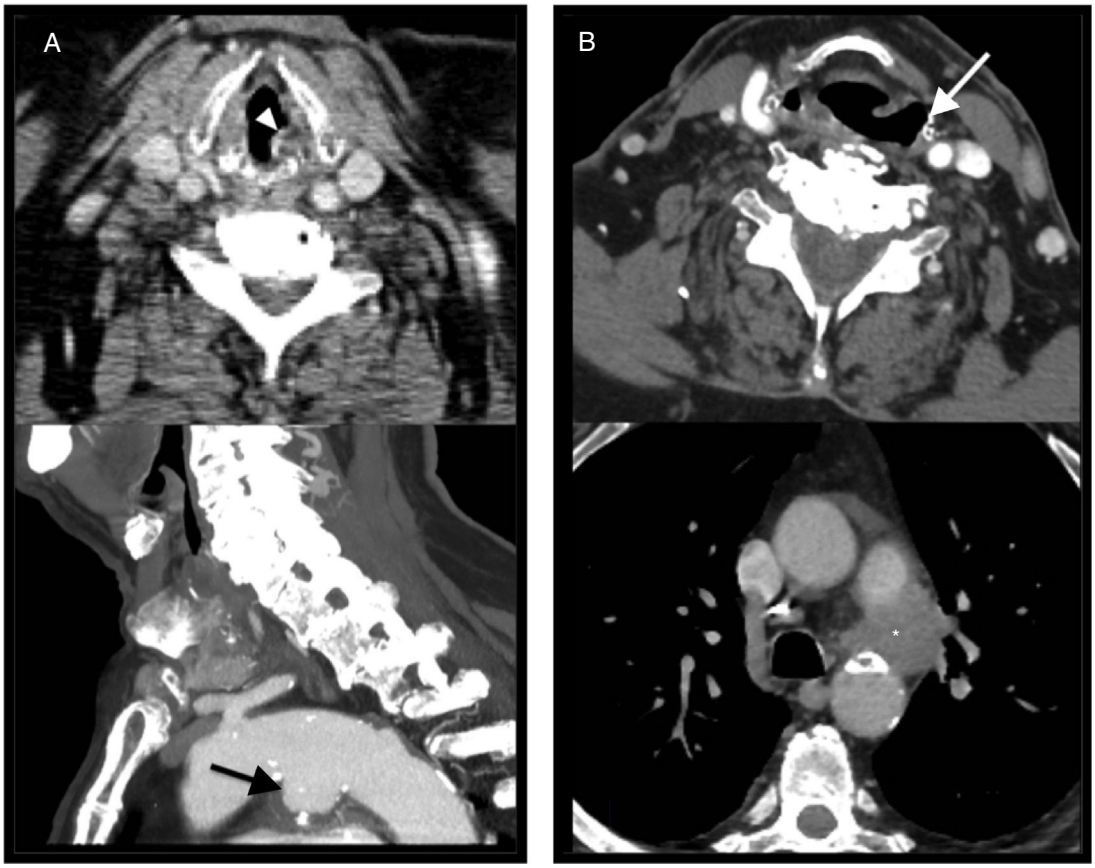

Figure 14 Cord paralysis. Left vocal cord paralysis. (A) Axial computed tomography image demonstrates medialization of the affected cord and anterior displacement of the ipsilateral arytenoid (arrowhead). (B) There is dilatation of the laryngeal ventricle and the pyriform sinus of the same side (arrow). When the paralysed cord is the left one, as in the cases shown, the study should extend to the aortopulmonary window. In the case of image A, the left cord paralysis is caused by a saccular aneurysm of the aortic arch (black arrow), whereas in the case of image B it is produced by a tumour mass in the aortopulmonary window (asterisk).

or abdominal neoplasms, compression by aortic aneurysm, cardiomegaly or TB sequelae.

In imaging, atrophy due to denervation of the proximal vagus is manifested by a decrease in the constricting muscles of the pharynx, and dilatation of the airway on the same side in the oropharynx and hypopharynx. More caudally, radiological findings are related to paralysis of the vocal cord (Fig. 14).

The technique of choice in suspected proximal vagal neuropathy is MRI, including in the study of the spinal cord and neck to the hyoid. When the vagal neuropathy is distal or peripheral, prior to direct otorhinolaryngological examination, a CT scan should be performed with intravenous iodinated contrast, exploring from the hyoid to the mediastinum; and even the carina in the case of left neuropathy.[16]

The *isolated involvement of the spinal accessory nerve (XI nerve pair)* occurs more commonly in the posterior triangle of the neck, after surgical interventions, by tumour or infectious infiltration (tuberculosis) of the cervical lymph nodes or trauma with shoulder dislocation. In the image, signs of denervation of the sternocleidomastoid or trapezius muscles can be observed (Table 2).[35]

The *isolated involvement of the hypoglossal nerve (XII nerve pair)* produces atrophy of the tongue. In cases of chronic atrophy, the most common findings on CT scan and MRI are fatty infiltration and prolapse of the tongue towards the oropharynx. It can be injured in the base of the skull (hypoglossal canal) by primary (chordomas or meningiomas) or metastatic tumours, and fractures of the occipital condyle, and, in the neck, by nasopharyngeal or lingual carcinomas, adenopathies or dissection of the internal carotid artery.[36]

Horner syndrome

It is produced by interruption of the oculosympathetic pathway. It is defined by the presence of miosis, ptosis (with apparent enophthalmos) and anhidrosis.

The aetiology depends on the place where the pathway formed by three neurons is affected:

- The 1st neuron (*central*) can be injured in the hypothalamus, brain stem (infarcts, demyelinating diseases) or in the cervical cord (trauma, tumours, syringomyelia, etc.).

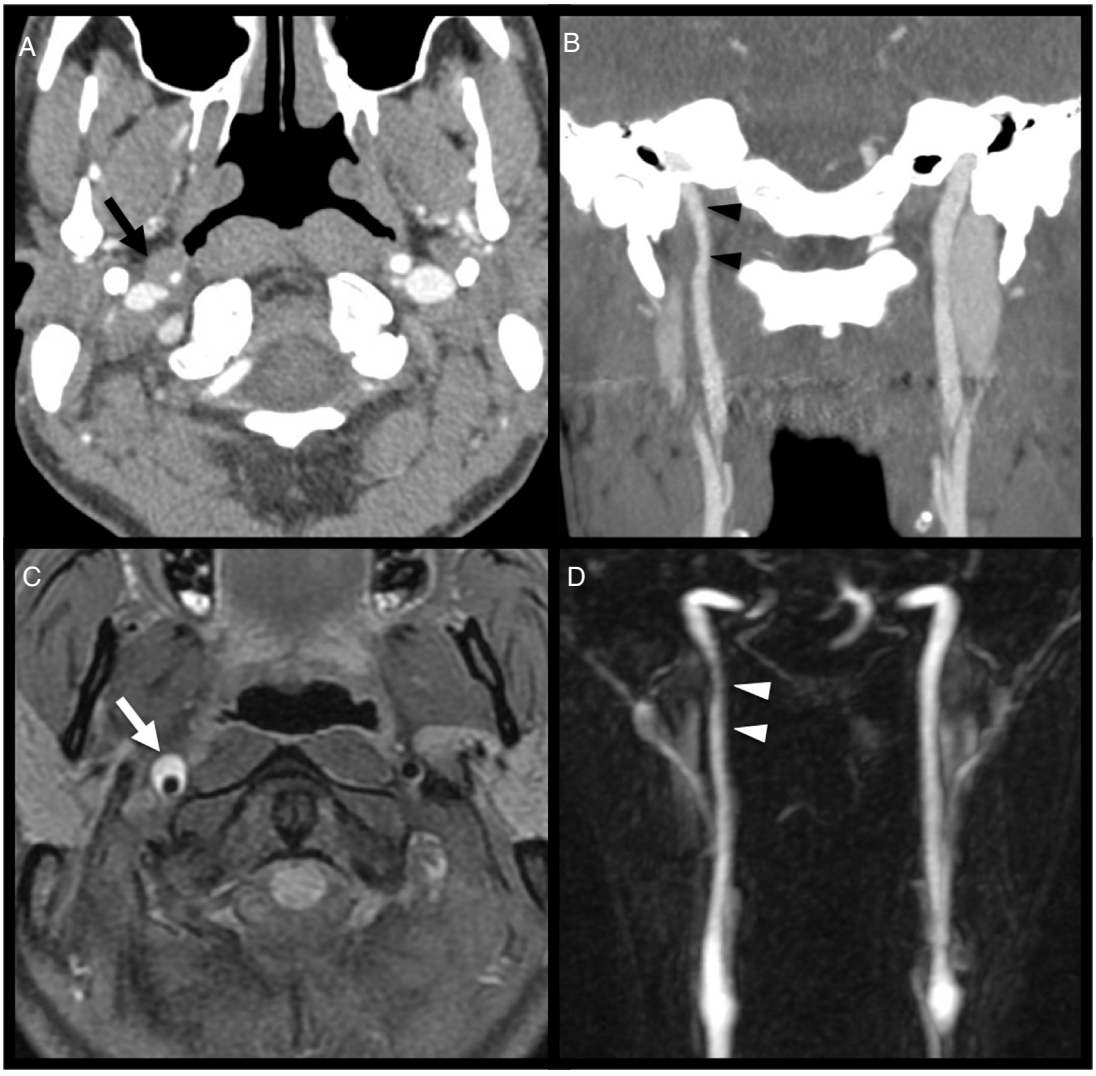

Figure 15 Carotid dissection. A 31-year-old male consulted for cervical pain and anisocoria. He refers to a history of physical effort a few days before. On examination, right Horner syndrome is found. Urgent CT angiography (A and B) shows a decrease in calibre of the right internal carotid artery in its distal cervical segment (black arrowheads) with suspicion of a haematoma on its wall (arrow). (C) The T1 axial image with fat suppression reveals a hyperintense crescent in the wall of the internal carotid artery (arrow) that corresponds to a subintimal haematoma characteristic of the carotid dissection. (D) The post-contrast 3D TOF angiography image is superimposable to the coronal reconstruction of the tomography with decreased calibre of the internal carotid artery (white arrowheads).

Brain MRI should be performed in patients with cerebral or brain stem symptoms.[37]

- The 2nd neuron (*preganglionic*) originates in the cervicothoracic cord (trauma, paravertebral tumours, spondylosis, etc.), reaches the sympathetic chain from the roots C8–T2 (lesions in the lower brachial plexus by traumatic avulsion, tumours of the apex pulmonary) and ascends to the superior cervical ganglion, close to the carotid bulb (thyroid carcinomas, surgery).
- In the absence of brain symptoms, MRI or CT scan studies should be directed to the neck, and cover the area from the angle of the jaw (superior cervical ganglion), or C2–C3 to T2.[37]
- The 3rd neuron (*postganglionic*) begins in the superior cervical ganglion. The vasomotor fibres and those destined for the sweat glands of the face ascend with the external carotid artery (lesions distal to the superior cervical ganglion do not produce facial anhidrosis). The remaining oculosympathetic fibres ascend with the internal carotid artery to the cavernous sinus, from where they reach their target organs transmitted by V1. Horner syndrome will be caused by any injury that dilates or compresses the internal carotid artery or exerts pressure on the carotid plexus. Among the most common causes are carotid dissection, cavernous sinus lesions and cluster headache. The examination of choice is MRI and angiography using MRI or CT scan (Fig. 15).[37]

Conclusions

The set of 12 pairs of cranial nerves constitutes a section of the highly complex nervous system, and is a diagnostic challenge both from a clinical and radiological point of view. Knowledge of anatomy and clinical orientation are crucial for the choice of the most appropriate study protocol and detection of the pathology. The imaging technique of choice for cranial nerve pathology is MRI, as it is the only technique that allows direct visualisation of the cranial nerves, supplemented, when necessary, by other techniques such as CT scan, ultrasound or angiography.

Authorship

1. Responsible for the integrity of the study: MJM.
2. Study conception: MJM.
3. Study design: MJM.
4. Data collection: MJM, SMM, JPE, JEV and MYF.
5. Analysis and interpretation of data: MJM, SMM, JPE, JEV and MYF.
6. Statistical processing: Not applicable.
7. Literature search: MJM, SMM, JPE, JEV and MYF.
8. Drafting of the paper: MJM, SMM, JPE, JEV and MYF.
9. Critical review of the manuscript with intellectually relevant contributions: MJM, SMM and MYF.
10. Approval of the final version: MJM, SMM, JPE, JEV and MYF.

Conflicts of interest

The authors declare that they have no conflicts of interest.

References

1. Blitz AM, Choudhri AF, Chonka ZD, Ilica AT, Macedo LL, Chhabra A, et al. Anatomic considerations, nomenclature, and advanced cross-sectional imaging techniques for visualization of the cranial nerve segments by MR imaging. Neuroimaging Clin N Am. 2014;24:1–15.
2. Blitz AM, Macedo LL, Chonka ZD, Ilica AT, Choudri AF, Gallia GL, et al. High-resolution CISS MR imaging with and without contrast for evaluation of the upper cranial nerves. Neuroimaging Clin N Am. 2014;24:17–34.
3. Amemiya S, Aoki S, Ohtomo K. Cranial nerve assessment in cavernous sinus tumors with contrast-enhanced 3D fast-imaging employing steady-state acquisition MR imaging. Neuroradiology. 2009;51:467–70.
4. Choi BS, Kim JH, Jung C, Hwang JM. High-resolution 3D MR imaging of the trochlear nerve. AJNR Am J Neuroradiol. 2010;31:1076–9.
5. Chagla GH, Busse RF, Sydnor BS, Rowley HA, Turski PA. Three-dimensional fluid attenuated inversion recovery imaging with isotropic resolution and nonselective adiabatic inversion provides improved three-dimensional visualization and cerebrospinal fluid suppression compared to two-dimensional flair at 3 tesla. Investig Radiol. 2008;43:547–51.
6. Fukuoka H, Hirai T, Shigematsu Y, Sasao A, Kimura E, Hirano T, et al. Comparison of the added value of contrast-enhanced 3D FLAIR and magnetization-prepared rapid acquisition of gradient echo sequences in relation to conventional postcontrast T1-weighted images for the evaluation of leptomeningeal diseases at 3T. AJNR Am J Neuroradiol. 2010;31:868–73.
7. Docampo J, Gonzalez N, Muñoz A, Bravo F, Sarroca D, Morales C. Neurovascular study of the trigeminal nerve at 3 T MRI. Neuroradiol J. 2015;28:28–35.
8. Meckel S, Maier M, Ruiz DS, Yilmaz H, Scheffler K, Radue EW, et al. MR angiography of dural arteriovenous fistulas: diagnosis and follow-up after treatment using a time-resolved 3D contrast-enhanced technique. AJNR Am J Neuroradiol. 2007;28:877–84.
9. Lutz J, Thon N, Stahl R, Lummel N, Tonn JC, Linn J, et al. Microstructural alterations in trigeminal neuralgia determined by diffusion tensor imaging are independent of symptom duration, severity and type of neurovascular conflict. J Neurosurg. 2016;124:823–30.
10. Ma J, Su S, Yue S, Zhao Y, Li Y, Chen X, et al. Preoperative visualization of cranial nerves in skull base tumor surgery using diffusion tensor imaging technology. Turk Neurosurg. 2016;26:805–12.
11. Abolmaali N, Gudziol V, Hummel T. Pathology of the olfactory nerve. Neuroimaging Clin N Am. 2008;18:233–42.
12. Binder DK, Sonne DC, Fischbein NJ. Olfatory nerve. In: Cranial nerves: anatomy, pathology imaging. New York: Thieme; 2010. p. 1–8.
13. Tseng J, Michel MA, Loehrl TA. Peripheral cyst: a distinguishing feature of estesioneuroblastoma with intracranial extension. Ear Nose Throat J. 2009;88:E14.
14. Ramdas S, Morrison D, Absound M, Li A. Acute onset blindness: a case of optic neuritis and review of childhood optic neuritis. BMJ Case Rep. 2016;2016.
15. Linn J. Cranial nerves. In: Naidich TP, Castillo M, Cha S, Smirniotopoulus JG, editors. Imaging of the brain. Philadelphia: Elsevier; 2012. p. 348–70.
16. Soldatos T, Batra K, Blitz AM, Chhabra A. Lower cranial nerves. Neuroimaging Clin N Am. 2014;24:35–47.
17. García-Rivera CA, Rozen TD, Zhou D, Allahyari P, Niknam R, Dougherty D, et al. Miller Fisher syndrome: MRI findings. Neurology. 2001;57:1755.
18. Kung NH, Van Stavern GP. Isolated ocular motor nerve palsies. Semin Neurol. 2015;35:539–48.
19. Chou KL, Galetta SL, Liu GT, Volpe NJ, Bennett JL, Asbury AK, et al. Acute ocular motor mononeuropathies: prospective study of the roles of neuroimaging and clinical assessment. J Neurol Sci. 2004;219:35–9.
20. Morrillon P, Bremmer F. Troclear nerve palsy. Br J Hop Med. 2017;78:C38–40.
21. Adams ME, Linn J, Yousry I. Pathology of the ocular motor nerves III, IV and VI. Neuroimaging Clin N Am. 2008;18:261–82.
22. Mark AS, Casselman J, Brown D, Sanchez J, Kolsky M, Larsen TC 3rd, et al. Ophthalmoplegic migraine: reversible enhancement and thickening of the cisternal segment of the oculomotor nerve on contrast-enhanced MR images. AJNR Am J Neuroradiol. 1998;19:1887–91.
23. Haller S, Etienne L, Kövari E, Varoquaux AD, Urbach H, Becker M. Imaging of neurovascular compressions syndromes: trigeminal neuralgia, hemifacial spasm. Vestibular paroxysmia, and glossopharyngeal neuralgia. AJNR Am J Neuroradiol. 2016;37:1384–92.
24. Veillon F, Ramos Taboada L, Abu Eid M, Rienm S, Debry C, Schultz P, et al. Pathology of the facial nerve. Neuroimaging Clin N Am. 2008;18:309–20.
25. Sismanis A. Tinnitus. Curr Neurol Neurosci Rep. 2001;1:492–9.
26. Lockwood AH, Salvi RJ, Burkard RF. Tinnitus. N Engl J Med. 2002;347:904–10.
27. Sonmez G, Basekim CC, Ozturk E, Gungor A, Kizilkaya E. Imaging of pulsatile tinnitus: a review of 74 patients. Clin Imaging. 2007;31:102–8.
28. Remley KB, Coit WE, Harnsberger HR, Smoker WR, Jacobs JM, McIff EB. Pulsatile tinnitus and the vascular tympanic

membrane: CT, MR and angiographic findings. Radiology. 1990;174:383–9.
29. Branstetter BF, Weissmann JL. The radiologic evaluation of tinnitus. Eur Radiol. 2006;16:2792–802.
30. Gultekin S, Celik H, Akpek S, Oner Y, Gumus T, Tokgoz N. Vascular loops at the cerebellopontine angle: is there a correlation with tinnitus? AJNR Am J Neuroradiol. 2008;29:1746–9.
31. McDermott AL, Dutt SN, Irving RM, Pahor AL, Chavda SV. Anterior inferior cerebellar artery syndrome: fact or fiction. Clin Otolaryngol. 2003;28:75–80.
32. Sirikci A, Beyacit Y, Ozer E, Ozkur A, Adaletli I, Cüce MA, et al. Magnetic resonance imaging based classification of anatomic relationship between the cochleovestibular nerve and anterior inferior cerebellar artery in patients with non-specific neuro-otologic symptoms. Surg Radiol Anat. 2005;27:531–5.
33. Nowé V, De Ridder D, Van de Heyning PH, Wang XL, Gielen J, Van Goethem J, et al. Does the location of a vascular loop in the cerebellopontine angle explain pulsatile and non-pulsatile tinnitus? Eur Radiol. 2004;14:2282–9.
34. Chadha NK, Weiner GM. Vascular loops causing otological symptoms. Clin Otolaryngol. 2008;33:5–11.
35. Bruno A, Policeni BA, Smoker WRK. Pathologic conditions of the lower cranial nerves IX, X, XI, and XII. Neuroimaging Clin N Am. 2008;18:347–68.
36. Smoker WRK. The hypoglossal nerve. Neuroimaging Clin N Am. 1993;3:193–206.
37. Reede DL, Garcon E, Smoker WRK, Kardon R. Horner's syndrome: clinical and radiographic evaluation. Neuroimaging Clin N Am. 2008;18:369–85.